Bimodal proton transfer in acid-base reactions in water

Matteo Rini
Max Born Institut fuer Nichtlineare Optik und Kurzzeitspektroskopie, Max Born Strasse 2A, D-12489 Berlin, Germany

Dina Pines, Ben-Zion Magnes, and Ehud Pines[a)]
Department of Chemistry, Ben-Gurion University of the Negev, P.O.B. 653, Beer-Sheva 84105, Israel

Erik T. J. Nibbering[a)]
Max Born Institut fuer Nichtlineare Optik und Kurzzeitspektroskopie, Max Born Strasse 2A, D-12489 Berlin, Germany

(Received 30 March 2004; accepted 13 August 2004)

We investigate one of the fundamental reactions in solutions, the neutralization of an acid by a base. We use a photoacid, 8-hydroxy-1,3,6-trisulfonate-pyrene (HPTS; pyranine), which upon photoexcitation reacts with acetate under transfer of a deuteron (solvent: deuterated water). We analyze in detail the resulting bimodal reaction dynamics between the photoacid and the base, the first report on which was recently published [M. Rini, B.-Z. Magnes, E. Pines, and E. T. J. Nibbering, Science **301**, 349 (2003)]. We have ascribed the bimodal proton-transfer dynamics to contributions from preformed hydrogen bonding complexes and from initially uncomplexed acid and base. We report on the observation of an additional $(6\ \mathrm{ps})^{-1}$ contribution to the reaction rate constant. As before, we analyze the slower part of the reaction within the framework of the diffusion model and the fastest part by a static, sub-150 fs reaction rate. Adding the second static term considerably improves the overall modeling of the experimental results. It also allows to connect experimentally the diffusion controlled bimolecular reaction models as defined by Eigen-Weller and by Collins-Kimball [D. Shoup and A. Szabo, Biophys. J. **40**, 33 (1982)]. Our findings are in agreement with a three-stage mechanism for liquid phase intermolecular proton transfer: mutual diffusion of acid and base to form a ''loose'' encounter complex, followed by reorganization of the solvent shells and by ''tightening'' of the acid-base encounter complex. These rearrangements last a few picoseconds and enable a prompt proton transfer along the reaction coordinate, which occurs faster than our time resolution of 150 fs. Alternative models for the explanation of the slower ''on-contact'' reaction time of the loose encounter complex in terms of proton transmission through a von Grotthuss mechanism are also discussed.
[DOI: 10.1063/1.1804172]

I. INTRODUCTION

A. General background

The dynamics of fast bimolecular reactions in solution have been subject of considerable interest to experimentalists and theoreticians for many years. Reactions of which the progress is influenced by the transport of reactants have been of particular interest in chemical, physical, and biological studies.[1–7] Investigation of these reactions have included proton[8–13] and electron transfer,[14,15] ion association-dissociation,[16] excimer formation,[17,18] dynamics of proteins,[19] enzymes, and membranes,[20] and fluorescence quenching.[3,7,21–24] It has been conventionally assumed that the reactants are transported and encounter each other by macroscopic diffusion and that the overall rate of bimolecular reactions is limited by diffusion. Generally speaking, diffusion-influenced bimolecular reactions may be viewed as made of two consecutive stages. The diffusion stage consists of movement of the reactants towards each other to the point where they encounter each other and form a reactive pair. The diffusive stage is followed by the reactive stage which takes place within the boundaries of the reaction (encounter) volume.

The first quantitative description of a diffusion-assisted reactive process was proposed by von Smoluchowski over 80 years ago in order to describe colloidal aggregation.[25] It models reactants as rigid spheres that react with unit probability upon mutual contact. The reactive configuration is defined by only one reaction parameter usually termed ''the contact (reaction) distance.'' Debye has generalized the von Smoluchowski model to include the important situation where reactants interact via a potential of a mean force $U(r)$.[26] For ionic reactants, $U(r)$ was approximated by the Coulomb potential leading to the well-known Debye–von Smoluchowski equation (DSE). The DSE was solved analytically for relatively long times after the time of initiation of the reaction by Hong and Noolandi.[27] Collins and Kimball[28] extended the model by incorporating a finite bimolecular reaction rate upon contact, k_0. The resulting reaction model is called the von Smoluchowski-Collins-Kimball (SCK) model.

a)Author to whom correspondence should be addressed.

No exact analytic solution of the SCK model with a Coulomb potential is known. Szabo utilized a Collins-Kimball type of boundary condition with a potential and derived an approximated expression for the time dependent reaction rate coefficient.[29] This expression can be easily implemented to interpret experimental data, which is the major advantage of the SCK model.

Both the DSE and the SCK formalisms result in a time dependent rate constant for diffusion assisted reactions; the rate constant decreasing from its early reaction-time value to its steady-state value. The time dependence of the rate constant is a consequence of relaxation of the separation-distance distribution between the reactants from its initial, nonreactive value to its steady-state (reactive) value.

Dynamic fluorescence quenching has been used many times as a probe for the transient effect of the time dependence of the reaction rate coefficient may be observed. Nemzek and Ware were first to observe the phenomenon of time-dependent fluorescence quenching rates in their pioneering work on fluorescence quenching in high viscosity solvents.[21] Combining time-resolved and steady-state measurements, they were also able to recover the ''static'' (nondiffusional) quenching rate. This static reaction part of a bimolecular reaction refers to the reaction rate of the fraction of the reactants, which at the onset of the reaction are at close proximity to each other, and so may react without diffusion. In experiments having limited time resolution the static reaction is a near δ function in time and its relative amplitude is governed by the separation distribution of the reactants in the ground state prior to the initiation of the reaction. In the event of direct complexation between the reactants, the relative amplitude of the static reaction is determined by the equilibrium constant of the complexation process.

The studies of diffusion-influenced electron-transfer reactions have usually employed time-correlated single photon counting and time-resolved phase modulation method (in which the time resolved emission is determined from the frequency response of the emission to intensity modulated light).[24] These fluorescence measurements have limited time resolution (typically, 30–90 ps instrument response time) relative to the extremely rapid electron transfer rate. The experimental results have been usually described by the SCK model with the transient part of the reaction masked in many occasions by the limited time resolution of the experiment.

Eads *et al.*[22] have used photon counting, fluorescence upconversion, and steady-state measurements to examine the quenching of rhodamine B by ferrocyanide. Neither the von Smoluchowski model nor the Collins-Kimball extension described the data well. Both the von Smoluchowski and Collins-Kimball boundary conditions assume that the reaction occurs only at a single separation distance and that the reaction rate is zero for all other separations. This is a very good approximation for proton transfer but fails to take into account the distance dependence of electron and energy transfers. A more satisfactory description of the data was achieved by incorporating a simple position-dependent sink model indicating a strong distance dependence for the reaction rate similar to the one found by Song *et al.*[30] Later on, Shannon and Eads examined the quenching of 7-amino-

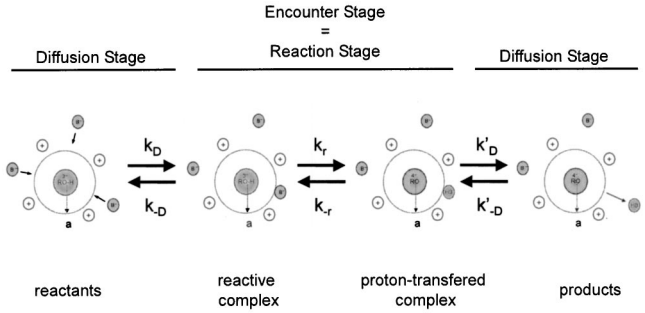

FIG. 1. Schematic drawing of the different stages of proton transfer according to the Eigen-Weller model. In the numerical estimation of the reaction rates it is assumed that the reaction partners are spherical and can interact at contact distance a in any direction along their spheres.

coumarin fluorescence by aniline and *N*,*N*-dimethylaniline in methanol.[23] They showed that the SCK model accurately described the 7-aminocoumarin/aniline system but not the 7-aminocoumarin/*N*,*N*-dimethylaniline system. Their analysis also showed that the electron transfer process exhibited a strong distance dependence on the donor-acceptor spatial separation and that it could be treated successfully using the Wilemski-Fixman approximation for the sink term.[31] Yabe *et al.* have more recently shown that even the von Smoluchowski model is adequate to describe the quenching of coumarin-15 with *N*,*N*-dimethylaniline at low concentrations. However, at higher concentrations the authors had to use an empirical potential between the donor and quencher to establish the spatial distribution of the quencher near the donor.[32]

A particular branch of diffusion-assisted bimolecular reactions of fundamental importance in chemistry and biology is the neutralization reaction between Brønsted acids and bases.[8–13,33] These reactions involve proton transfer, a key process in elementary phenomena such as acid-base neutralization and enzymatic reactions,[20] the abnormal high proton mobility in aqueous solutions,[34] the autoionization in water,[35] and proton pumps through membrane protein channels.[36] According to Eigen and co-workers[11,12] and Weller[2,9,10] reversible general acid-base reactions in solution are diffusion assisted and may be generally modeled by an overall three-step reaction scheme consisting of a two-stage proton transfer scheme at each side of the acid-base equilibrium (Fig. 1). Each of the two-stage proton transfer reaction is made of (1) diffusional motion, where the acid and base approach each other to form an encounter pair when the mutual distance equals the reaction contact radius, and by (2) intrinsic (contact) proton transfer. Each one-side proton-transfer reaction is completed by subsequent separation of the products by diffusion (3). Theoretical studies have focused on the actual (contact) proton-transfer event, reaction stage (2), and have tackled questions such as whether the reaction rate is determined by activated dynamics of the proton over a reaction barrier[37–39] or by proton tunneling motion through the barrier[40] or a mixture of the two processes, and the extent of the role of solvent in determining the reaction coordinate.[41]

Within the framework of the Eigen-Weller model, the

intrinsic proton transfer rates have been assumed to lie in the range of $(10\ \text{ps})^{-1}$–$(1\ \text{ps})^{-1}$ with a typical reaction contact radius of 5–8 Å. However, diffusion rates are typically much slower than the on-contact proton transfer rates, so the direct observation of the actual proton transfer reaction dynamics between freely diffusing acid and base molecules in liquid solutions has remained problematic. Moreover, the role of the solvent in the acid-base encounter pair remains to be solved, in particular with respect to the observed intrinsic intermolecular proton transfer rates which have been found to be at least one order of magnitude slower than the characteristic time scale of intramolecular hydrogen and proton transfer reactions in many molecular systems following electronic excitation; many of them having typical time constants on the order of 100 fs.[42]

At low concentrations, acid-base pairs are formed by bimolecular encounters of which the frequency is controlled by diffusion. The encounter rates are typically much slower than the on-contact proton transfer rates, so the direct measurement of the actual (contact) proton transfer reaction has been one of the basic objectives in acid-base chemistry.[2,9,10] The obvious way to eliminate the dominating (rate-limiting) diffusion stage is by studying acid-base pairs in direct contact to each other. This strategy for the elucidation of the intrinsic bimolecular reaction mechanisms has been used before in time-resolved studies of low temperature gas-phase clusters[43–56] and in liquid solution.[57–65] In the case of room temperature liquid solutions, however, one always has to consider the possibility of a variety of conformations when the reaction partners are associated to each other. This could lead to situations where the reaction partners are oriented in less favorable geometries, and as a result the reaction coordinate is not formed. A distribution in relative orientations will even take place in the case of electron transfer from an electron donating solvent to an electron acceptor,[66–71] and as such it remains to be resolved how the reaction coordinate is composed when electron donor and acceptor are nearest neighbors. In the case of hydrogen-bonded complexes in nonpolar solvents the proton transfer reaction coordinate is formed when the acid-proton–donating and base-proton–accepting groups are directly connected to each other by a hydrogen bond.[59–61] In protic self-associate solvents such as water it could well be that, besides a fraction of directly bound acid-base complexes, another fraction of the associated acid-base complexes may be temporarily connected to each other through a water wire, i.e., one or several water molecules connecting the acid-proton–donating and the base-proton–accepting groups via a continuous network of hydrogen bonds. In this context we also refer to an elegant cluster experiment on 7-hydroxyquinoline-$(NH_3)_3$, where proton donating and accepting groups are connected by a wire of ammonia molecules.[54]

Pines and co-workers[72] made an attempt to directly measure the intrinsic proton transfer rate at reaction contact of several naphthol- and pyrenol-type photoacids and several types of carboxylic bases in aqueous solution. In the ground state, these acid-base pairs are unreactive. They are linked by a network of intermolecular hydrogen bonds along which the proton transfer reaction eventually occurs when an optical trigger pulse switches the acidity of the photoacid by 5–9 units of pK_a (where K_a is the acidity constant of the photoacid in the ground state). Such excited state proton-transfer reactions were measured at $1M$ and $8M$ concentrations of the carboxylic base.[72] The time resolution of the experiments was limited by the time response of the single-photon-counting apparatus (17–22 ps). The conclusion was that the intrinsic proton-transfer rate may be estimated directly in very high concentrations ($8M$) of a complexing Brønsted base, thus circumventing the limitation imposed by diffusion. Pines *et al.* also analyzed the proton-transfer rates in the solutions containing $1M$ of carboxylates, by considering a two-stage bimolecular reaction scheme, based on the Eigen-Weller model. They showed that the bimolecular rates measured in the most exothermic proton-transfer reactions appear to be larger than their steady-state values. However, the expected time dependence of the reaction rate constants was masked by the parallel proton-transfer reaction from the photoacid to the solvent and by the limited time resolution of the single-photon-counting apparatus. Consequently, the need for more refined experiments having better time resolution was recognized and called upon.

Using the technique of femtosecond UV-pump-VIS probe, Genosar *et al.*[73] have utilized one of the reactive systems that had been previously investigated by Pines *et al.*[72] and measured the proton-transfer reaction of the photoacid [8-hydroxy-1,3,6-trisulfonate-pyrene (HPTS)], at the concentration range of $(0.5–4)M$ of sodium acetate in water. Values of $1.6\times10^{11}M^{-1}\,\text{s}^{-1}$ and $4\times10^{10}M^{-1}\,\text{s}^{-1}$ for the intrinsic bimolecular proton transfer rate between photoexcited HPTS and acetate in H_2O and D_2O, respectively, were extracted using the SCK approach. These values are significantly larger than the corresponding diffusion-limited rate constants of the reaction that were measured at long times,[72,73] and with the increased time resolution the overall bimolecular reaction rates were found indeed to be time dependent. Although very fast transients on the time scale of several hundred femtoseconds to a few picoseconds were also observed by Genosar *et al.* they were identified as emerging from the ultrafast solvation dynamics of the photoacid and from excited-state absorption contributions to the pump-probe signal.[73]

To better explore the nature of the nonexponential (transient) kinetics in acid-base reactions Cohen *et al.*[74,75] conducted single-photon-counting measurements between a photoacid, 2-naphthol-6-sulfonate, and high concentrations of acetate base in a medium of high viscosity (water-glycerol mixtures) to slow down the diffusion by roughly a factor of 40 as compared to that in pure water. Marked nonexponentiality of the reaction rate was observed and the kinetics were adequately described by the SCK model.

The experiments by Pines *et al.*,[72] Genosar *et al.*,[73] and Cohen *et al.*[74,75] have demonstrated that application of optical spectroscopy imposes limitations on the outcome when applied to study proton-transfer dynamics.[76] The unparalleled sensitivity and dynamic range of the single-photon-counting technique is countered by its limited time resolution. Pump-probe measurements are often complicated by the strong overlap of different contributions (bleach, stimu-

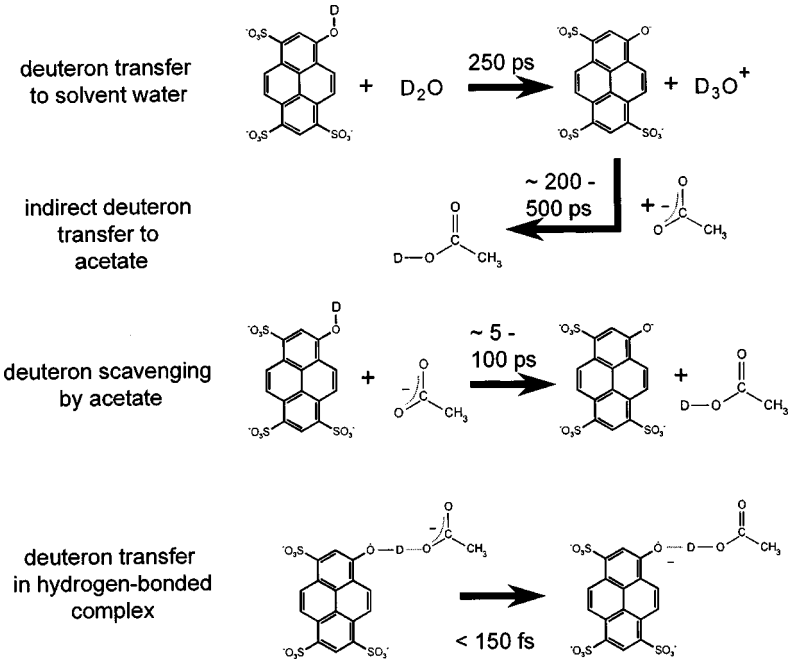

FIG. 2. Possible deuteron transfer reaction steps that play a role in the acid-base neutralization of HPTS and acetate in deuterated water, as investigated in this study. At the lowest concentrations (0.25*M* acetate) HPTS transfers its deuteron to water, to be followed by deuteron pickup by the acetate. At higher base concentrations ($>1M$ acetate) acetate scavenges the deuteron directly from HPTS. In the highest base concentrations used in this study direct complexes between HPTS and acetate exist before photoexcitation, which will promptly transfer the deuteron after photoinitiation of the reaction.

lated emission, and excited state absorption) to the pump-probe signal.[77] Moreover, in condensed phase studies, electronic transitions are usually strongly affected by excess vibrational excitation, intramolecular vibrational redistribution, and vibrational cooling (vibrational energy dissipation to the solvent)[78–84] and solvent reorganization (solvation dynamics),[85–87] which may mask the ultrafast dynamics of the proton-transfer process. Time-resolved mid-IR spectroscopy with femtosecond time resolution has the advantage of being largely free of the above-mentioned limitation of conventional time-resolved optical spectroscopy. It has thus become our technique of choice in pursuing contact proton transfer in bimolecular acid-base reactions.

B. The observation of bimodal proton transfer rates by femtosecond-resolved mid-IR spectroscopy

Recently, we have reported on femtosecond-time-resolved measurements of acid-base reactions using optical pump and mid-infrared (mid-IR) probe spectroscopy.[88] Specific infrared active vibrational marker modes were followed at the proton-donor (photoacid) and proton-acceptor (carboxylate) sides. We have used the benchmark photoacid HPTS (Refs. 72 and 73), which served as an ultrafast optical switch for the IR-probed proton-transfer reaction. We have used concentrated solutions of a carboxylate base, the acetate anion, which was the proton acceptor,[72] a reaction condition introduced by Pines *et al.*,[72] and the solvent was deuterated water (Fig. 2). We observed a bimodal proton-transfer rate: a sub−150 fs reaction component (that has not been reported before) is followed by a nonexponential part found to be at least one order of magnitude slower than the first one. The time behavior of the slower reaction component was found to be in general agreement with the previous reports on the same reaction.[72,73] Its time dependence was treated using the SCK model.[73] We have attributed these two time components to dynamics of the two fractions of directly and indirectly interacting acid-base molecules, respectively. Using both IR and optical spectroscopies we have demonstrated that a significant fraction of acid-base pairs is directly linked by a hydrogen bond already in the ground state of the photoacid in concentrated acetate solutions.

Only after an optical trigger pulse, the deuteron transfer reaction is initiated from the HPTS to the acetate base along this preexisting hydrogen bond. We have attributed the ultrafast reaction dynamics, observed to be faster than the experimental time resolution of 150 fs, to deuteron transfer in ''tight'' hydrogen-bonded HPTS-acetate complexes $\mathrm{ROD}\cdots\mathrm{B}^- \rightarrow \mathrm{RO}^-\cdots\mathrm{DB}$ without intermediate water molecules. The remaining part of the acid-base population reacted in a diffusion-assisted fashion which was modeled by the SCK reaction mechanism.[29,73–75] In accordance with previous observations,[72–75] the diffusion-assisted reaction was found to be much slower, with an intrinsic on-contact reaction time constant on the order of several picoseconds. Our observation of bimodal reaction dynamics reveals a paradigm. We have found a much faster reaction rate for acid-base pairs in direct contact than what is predicted when analyzing the reaction dynamics of the fraction governed by diffusional motion. The significant difference in the reaction time scales can only be reconciled into one picture by assumption of an extra, inner sphere, reaction stage in acid-base reactions in aqueous solutions that has not been observed before and was accessed by using concentrated solutions of a proton acceptor. Our results have thus called for a refinement of the traditional Eigen-Weller picture for low-concentration acid-base reactions in aqueous solutions.[88]

C. Outline of the paper

In this contribution we aim to unify the reaction model for acid-base reactions at low and high concentrations by considering the outcome of femtosecond mid-infrared (mid--

IR), steady-state and single-photon-counting UV-VIS spectroscopic methods. We report on the existence of a static component of 6 ps in the proton-transfer reaction between HPTS and acetic base at high acetate concentrations, which is almost two orders of magnitude slower than the sub–150 fs component we have reported before and attributed to acid-base complexes directly linked by a hydrogen bond.[88] We attribute this additional 6 ps component to the fraction of the acid-base contact pairs which are weakly interacting and are formed in the ground state of the photoacid in concentrated acetate-base solutions. These preexisting contact pairs are akin to the contact pairs formed by diffusion in dilute solutions of the acetate base. In agreement with the above reaction model, we report on the correspondence, between this static (pseudo-unimolecular) proton-transfer rate and the intrinsic (bimolecular) reaction rate constant k_0, we have found by analyzing the diffusional part of the same proton transfer reaction by using the SCK formalism.

The paper is organized as follows. In Sec. II we consider the relation between the unimolecular Eigen-Weller reaction constant and the bimolecular Collins-Kimball intrinsic reaction constant and summarize the relevant equations for data analysis, including the dependence of the signals on the relative polarization of the UV-pump and IR-probe pulses. In Sec. III we describe the details of the experimental methods used. In Sec. IV we compare the time-resolved data with predictions of the kinetic model. We outline in Sec. V a general three-stage kinetic model of proton transfer between Brønsted acids and Brønsted bases. This model is in the spirit of the model for general acid-base reactions which was previously considered by Bell briefly in his book on the tunnel effect[89] and was attributed by him to be largely based on the work of Marcus.[90,91] In Bell's words the acid and base form first ''the encounter complex in which the reactants have come together, but do not interact appreciably and have not undergone any significant modification of their solvation shells.'' The next reaction stage occurs with ''the conversion of the encounter complex into the reaction complex in which the reactants and the neighboring solvent molecules are in positions and orientations favorable to proton transfer'' and the actual proton transfer takes place within the reaction complex. In this study we discuss in detail several possible mechanisms of a three-stage proton-transfer reaction, which are based on our observation of the bimodal proton-transfer reaction between the HPTS acid and the acetate base.

II. RELATIONSHIP OF COLLINS-KIMBALL MODEL TO THE EIGEN-WELLER TWO-STEP PROTON-TRANSFER SCHEME

A. Two-stage bimolecular proton-transfer reaction scheme

We start by considering the Eigen-Weller (EW) two-stage bimolecular proton-transfer reaction as outlined from the reactant side (scheme 1; Fig. 1).

Reactants (Diffusion stage)		Reactive-complex (Encounter stage)		Proton-transferred complex (Product stage)
ROH+B	$\underset{k_{-D}}{\overset{k_D}{\rightleftarrows}}$	$(RO-H\cdots B)_a$	$\underset{k_{-r}}{\overset{k_r}{\rightleftarrows}}$	$(RO^-\cdots{}^+H-B)_a$

Scheme1

ROH and B are the acid and base, respectively. k_D and k_{-D} are diffusion-limited reaction rates for the encounter and separation of the reactive complex, and k_r and k_{-r} are the unimolecular constants for the intrinsic proton-transfer rates at the contact separation a.

Making the steady-state approximation for the concentration of the complex, the effective overall bimolecular rate constant of the proton-transfer reaction, k_f,[92] is given by

$$k_f=\frac{k_D k_r}{k_r+k_{-D}}. \tag{1}$$

B. SCK model of diffusion-influenced reaction with a screened Coulomb potential

We outline below the SCK model[25–28] of diffusion-influenced reactions with the radiative boundary at the contact distance a, where the time-dependent second-order (bimolecular) rate coefficient $k(t)$ is obtained from the flux of the incoming reactants across the surface of the contact sphere as defined by the closest approach (contact) distance:

$$k(t)=4\pi Da^2\left.\frac{\partial\rho}{\partial r}\right|_{r=a}\Big/\, c_0. \tag{2}$$

We consider the particular case of large excess of proton acceptors (acetate ions) over the proton donors (photoacid), ρ the density of proton acceptors with respect to a single, central proton donor. c_0 is the average concentration of the proton acceptor and D is the relative diffusion coefficient between the two reactants, approximated by the sum of their respective diffusion coefficients, $D=D_{\mathrm{Ac}^-}+D_{\mathrm{HPTS}}$.

The time dependence of the concentration gradient of the proton acceptor is assumed to behave according to the DSE:[25–26]

$$\frac{\partial c(r,t)}{\partial r}=r^{-2}\frac{\partial}{\partial r}Dr^2e^{-\beta u(r)}\frac{\partial}{\partial r}e^{\beta u(r)}c(r,t), \tag{3}$$

where $U(r)$ is the interaction potential as function of distance r, and $\beta=1/k_BT$, with k_B the Boltzmann's constant and T the absolute temperature.

In the SCK approach[28] the reaction flux at contact is assumed to be proportional to the local reactant concentration at contact. The proportionality constant k_0 is the intrinsic (bimolecular) rate constant of the reaction upon contact. In passing and to be further discussed below, we note that k_0 should relate to the on-contact unimolecular rate constant k_r of the Eigen-Weller fame of reaction, Scheme 1. In the SCK model the partially absorbing (radiative) boundary condition is given by

$$4\pi Da^2\frac{\partial\rho}{\partial r}=k_0c(a). \tag{4}$$

For the case of $U(r)=0$, the DSE was solved by Collins and Kimball:[28]

$$k(t)=\frac{k_{SD}k_0}{k_{SD}+k_0}\left[1+\frac{k_0}{k_{SD}}\exp(\gamma^2 Dt)\operatorname{erfc}(\sqrt{\gamma^2 Dt})\right], \quad (5)$$

with the diffusion rate constant k_{SD}:

$$k_{SD}=4\pi NDa, \quad (6)$$

and

$$\gamma=a^{-1}\left[1+\frac{k_0}{k_{SD}}\right], \quad (7)$$

where k_{SD} is the diffusion-limited second-order rate constant for steady-state conditions at long times after initiation of the reaction, N is Avogadro's number, and erfc means complementary error function.

For a Coulomb potential it is not possible to solve the DSE analytically using the SCK boundary condition. The analytic approximation of Szabo[29] for the time dependent rate constant is

$$k(t)=\frac{k_{SD}k_0e^{-\beta U(a)}}{k_{SD}+k_0e^{-\beta U(a)}}\left[1+\frac{k_0e^{-\beta U(a)}}{k_{SD}}\times\exp(\gamma'^2 Dt)\operatorname{erfc}(\sqrt{\gamma'^2 Dt})\right], \quad (8)$$

with the steady-state diffusion rate constant k_{SD} now given by

$$k_{SD}=4\pi DNa_{\text{eff}}, \quad (9)$$

and

$$\gamma'=a_{\text{eff}}^{-1}\left[1+\frac{k_0e^{-\beta U(a)}}{k_{SD}}\right]. \quad (10)$$

The effective radius a_{eff} is defined as

$$a_{\text{eff}}^{-1}=\int_0^\infty e^{\beta U(a)}r^{-2}dr. \quad (11)$$

The first term in Eq. (8) determines the asymptotic value reached at long times, which is the steady-state SCK reaction rate constant:

$$k_{\text{SCK}}^{SS}=\frac{k_{SD}k_0e^{-\beta U(a)}}{k_{SD}+k_0e^{-\beta U(a)}}, \quad (12)$$

and the second term describes the transient value of the reaction constant. For reactions where the reaction rate constant on contact, $k_0e^{-\beta U(a)}$, is much larger than the diffusion-limited rate constant k_{SD}, one finds that the initial reaction rate constant immediately following the onset of the reaction is $k_0e^{-\beta U(a)}$. The initial reaction rate constant decreases with the progress of the reaction until it reaches its steady-state value at long times, $k(\infty)=k_{\text{SCK}}^{SS}$. Both the initial and the steady-state rate constants are bimolecular rate constants. In the event of one of the reactants in large excess over the other, the pseudo- first-order reaction rate constants at these limits are $c_0k_0e^{-\beta U(a)}$ and $c_0k_{\text{SCK}}^{SS}$, respectively, where c_0 is the concentration of the reactant in excess.[22,23,73]

C. Relation between bimolecular reaction constant k_0 of Collins-Kimball and unimolecular constant k_r in the Eigen-Weller reaction model

While the intrinsic proton-transfer rate constant k_r of the EW model (Scheme 1; Fig. 1) obeys detailed balancing and is readily recognized as being part of the overall equilibrium constant of the reaction:

$$K_{eq}^{ov}=k_{-r}k_{-D}/k_rk_D; \quad (13)$$

this is not immediately so with the intrinsic bimolecular rate constant k_0 of the SCK model. The relation between the bimolecular reaction constant k_0 and the unimolecular reaction constant k_r was first established by Shoup and Szabo.[93] Closely following the derivation appearing in Ref. 93, we consider φ_{CK}, the probability that reactants in the SCK model generated at contact are actually reacting. Shoup and Szabo showed that the steady-state SCK reaction rate constant k_{SCK}^{SS}, given by Eq. (12), is just the diffusion-limited rate constant k_{SD} times φ_{SCK}, the probability that reactants at contact form a complex and eventually react:

$$k_{\text{SCK}}^{SS}=k_{SD}\varphi_{\text{SCK}}, \quad (14)$$

or

$$\varphi_{\text{SCK}}=\frac{k_{\text{SCK}}^{SS}}{k_{SD}}. \quad (15)$$

We have defined the reaction complex in the EW reaction model as $(\text{RO-H}\cdots\text{B})_a$ (Scheme 1; Fig. 1). The probability that this complex reacts is

$$\varphi=\frac{k_r}{k_r+k_{-D}}. \quad (16)$$

Following Ref. 93, we equate φ [Eq. (16)] with φ_{SCK} of Eq. (15). It may be done in a unique way when the following correspondences exist between the SCK and the EW reaction models:

$$k_{SD}=k_D, \quad (17)$$

and

$$k_0e^{-\beta U(a)}=\frac{k_D}{k_{-D}}k_r=K_{eq}k_r, \quad (18)$$

meaning that the second-order rate constant k_0 of the SCK model is proportional to the equilibrium constant for the formation of the reactive complex, K_{eq}, times the first-order rate constant of the EW model for the proton transfer within the acid-base complex k_r.

The equilibrium constant for the formation of the reaction complex can be written as[93]

$$k_D/k_{-D}=K_{eq}=\frac{4\pi a^3}{3}Ne^{-\beta U(a)}, \quad (19)$$

which is Fuoss's equation for the equilibrium partition constant between contact-separated and infinitely separated ion pairs.[94] N is the number of particles present in 1 cm^3 of a 1M solution of particles and is sometimes referred to as the Avogadro's number per mM. Substituting this value of K_{eq} in Eq. (19) we finally relate the bimolecular proton-transfer

rate constant k_0 of the SCK model to the unimolecular proton-transfer rate constant within the EW reaction complex:[93]

$$k_0=\frac{4\pi a^3}{3}Nk_r, \tag{20}$$

so k_r of the EW reaction model is equal to k_0 of the SCK reaction model multiplied by the relative concentration of the reaction pair at contact separation. At very high concentrations the physical meaning of the two intrinsic reaction constants may diverge if $c_0k_0e^{-\beta U(a)}$ is larger than k_r. To be consistent with the EW reaction model the (concentration dependent) bimolecular reaction rate inherent to the SCK model can only approach k_r but not exceed it when the bimolecular reaction probability approaches unity. Equivalently, according to the EW model the maximum concentration of the reactive pair at contact is $1/[(4/3)\pi a^3N]$ to obey detailed balancing. However, there is no such a constraint in the SCK model, where the effective concentration of the reactants on contact may assume any value depending on the bulk concentration and interaction potential used.

D. The survival probability of the proton donor in presence of an excess concentration of proton acceptor

The survival probability $S_{\mathrm{ROH}}(t)$ of a proton donor ROH*, surrounded by an equilibrium distribution of proton-acceptor molecules with the initial condition $S(0)=1$, may be approximated according to the following kinetic equation:

$$\frac{dS_{\mathrm{ROH}}(t)}{dt}=-c_0k(t)S_{\mathrm{ROH}}(t)-k_wS_{\mathrm{ROH}}(t), \tag{21}$$

where k_w is the first-order dissociation constant of the proton donor (acid) to the solvent, and c_0 is the bulk concentration of the proton acceptor. $k(t)$ is the time-dependent rate coefficient given by Eq. (5).

Integrating, the survival probability of the acid is given by

$$S_{\mathrm{ROH}}(t)=\exp\left[-k_wt-\int_0^t c_0k(t')dt'\right]. \tag{22}$$

For the corresponding rise of the photobase (RO^-) population one has

$$S_{\mathrm{RO}^-}(t)=1-\exp\left\{-k_wt-\int_0^t c_0k(t')dt'\right\}. \tag{23}$$

For very high concentrations of proton acceptor when proton transfer almost exclusively occurs by the direct reaction between the photoacid and the base $[k_w\ll\int_0^t k(t')dt']$ the decay of the photoacid is given by

$$S_{\mathrm{ROH}}(t)=\exp\left\{-c_0\int_0^t k(t')dt'\right\}, \tag{24}$$

and the corresponding rise in the population of the photobase is

$$S_{\mathrm{RO}^-}=1-\exp\left\{-c_0\int_0^t k(t')dt'\right\}. \tag{25}$$

The integral of $k(t)$, derived from Eq. (5), has the following form in the absence of an interaction potential because of very effective screening [setting $U(r)=0$]:

$$\int_0^t k(t')dt'=\frac{k_{SD}k_0}{k_{SD}+k_0}\left\{t+\frac{k_0}{k_{SD}D\gamma^2}[\exp(\gamma'^2Dt)\times\mathrm{erfc}(\sqrt{\gamma^2Dt})+2\sqrt{\gamma^2Dt/\pi}-1]\right\}. \tag{26}$$

For a screened Coulomb potential it was found[22,23] that

$$\int_0^t k(t')dt'=\frac{k_{SD}k_0e^{-\beta U(a)}}{k_{SD}+k_0e^{-\beta U(a)}}\left\{t+\frac{k_0e^{-\beta U(a)}}{k_{SD}D\gamma'^2}[\exp(\gamma'^2Dt)\times\mathrm{erfc}(\sqrt{\gamma'^2Dt})+2\sqrt{\gamma'^2Dt/\pi}-1]\right\}. \tag{27}$$

In our experiment, we approximate the potential between the photoacid (HPTS) and the proton-base (acetate) by the Debye-Hückel (DH) ionic screening law similar to the procedure outlined in Refs. 73 and 95:

$$U(r)/k_BT=\frac{R_D}{r}\frac{e^{-\kappa_{\mathrm{DH}}(r-a)}}{1+a\kappa_{\mathrm{DH}}}, \tag{28}$$

with

$$R_D=z_1z_2e^2/\epsilon k_BT \tag{29}$$

and

$$\kappa^2=8\pi e^2I/\epsilon k_BT, \tag{30}$$

where k_B is Boltzmann's constant, a is the contact radius, ϵ is the permittivity of the solution, e is the elementary charge, κ^{-1} is the screening length, and I is the ionic strength, which in our case is practically equal to the acetate concentration, and $z_1=-1$, $z_2=-3$ are the charge numbers of the acetate and HPTS, respectively.

E. The survival probability of the proton acceptor

In this study we are able to follow the proton-transfer kinetics both from the photoacid side and the base side. In order to describe the kinetics of the acetate base we assume that any excited photoacid will ultimately transfer its proton either to the solvent (water) or to the proton base, where any proton released to the solvent eventually will be picked up by the base (proton scavenging by the base).[96,97] The survival probability of the released proton (deuteron) following acid dissociation to the solvent is given by

$$\frac{dS_{\mathrm{H}^+}}{dt}=k_wS_{\mathrm{ROH}}(t)-k_{dl}cS_{\mathrm{H}^+}. \tag{31}$$

At high concentration of base the largest fraction of photoacid transfers its proton directly to the base. The small fraction of proton transfer via the indirect route of acid dissociation to the solvent and then proton pick-up by the base in a

diffusion-limited reaction may be approximated by the diffusion-limited rate constant of the reaction, k_{dl};[96,97]

$$k_{dl}=4\pi D' a'_{\mathrm{eff}} N, \tag{32}$$

where $U(r)/k_BT$ is defined in a similar fashion as in Eq. (28) and a'_{eff} is given by Eq. (11) and D' is the relative diffusion coefficient between the base and the solvated proton.

Finally, the survival probability of the protonated base (H^+Ac) is given by

$$\frac{dS_{H^+Ac}}{dt}=c_0k(t)S_{\mathrm{ROH}}(t)+c_0k_{dl}S_{H^+}. \tag{33}$$

The differential equations for the survival probabilities S_{H^+} and S_{H^+Ac} [Eqs. (31) and (33)] may be solved analytically:

$$S_{H^+}=\exp(-c_0k_{dl}t)\int_0^t S_{\mathrm{ROH}}(t')k_w\exp(c_0k_{dl}t')dt', \tag{34}$$

$$S_{H^+Ac}=\int_0^t [c_0k(t')S_{\mathrm{ROH}}(t')+c_0k_{dl}S_{H^+}]dt'. \tag{35}$$

Using the expression for survival probability of $S_{\mathrm{ROH}}(t)$, Eq. (22), we have integrated equations (34) and (35) numerically to find the survival probability for proton acceptor. At high concentration of base the proton transfer occurs almost exclusively by direct proton transfer reaction between the acid and the base [$k_w \ll \int_0^t c_0k(t')dt'$ and $S_{H^+}=0$]. Thus, under such conditions the rise of the protonated form of the proton acceptor follows the rise of the conjugated anion of the acid (photobase) [Eq. (25)] and is given by Eq. (25a):

$$S_{H^+Ac}=1-S_{\mathrm{ROH}}(t)=1-\exp\left\{-c_0\int_0^t k(t')dt'\right\}. \tag{25'}$$

F. Polarization-dependent signals and anisotropy decay

When performing UV-pump IR-probe spectroscopy with linearly polarized pulses one has to take into account the fact that the electronic and vibrational transition moments can be pointing to different directions in the molecular frame. This may lead to pump-probe signals that are polarization dependent. In addition, since the diffusion-controlled proton-transfer dynamics occur in our experiments with a time scale similar to that of rotational motions in room temperature liquids (several picoseconds up to 1 ns), these anisotropic signals may be affected by rotational diffusion. As a result we have taken this into account by assuming that HPTS, in both photoacid and photobase form, is a symmetric rotor, and that for both forms the rotational diffusion axes, as well as rotational diffusion time constant do not change upon the transfer of a proton/deuteron. In this simplified case we can use a simple expression for the time-dependent rotational anisotropy $r(t)$:

$$r(t)=\tfrac{2}{5}P_2[\cos(\lambda)]\exp(-t/6D_{rot}), \tag{36}$$

where the rotational correlation time τ_{rot} is connected to the rotational diffusion time constant D_{rot} through the relation $\tau_{rot}=1/(6D_{rot})$, and the $P_2(x)$ denotes the second-order Legendre polynome of x. The anisotropy is described the angle λ between the optical transition dipole moment of HPTS photoacid and the infrared transition dipole moment of either photoacid or photobase vibrational bands. In reality the expression for the rotational anisotropy of HPTS, being in fact an asymmetric rotor, is more complex, consisting of five different exponentially decaying functions, and several products of direction cosines of the optical and infrared transition dipoles with respect to the principal rotation axes.[98] In addition, one has to include in general the possibility of different rotational principal axes for photoacid and photobase species, as well as different rotational diffusion constants.[99] Since both photoacid and photobase species form a similar number of hydrogen bonds with the solvent through the sulfonate and C-O groups, the structure is almost equal, and the mass is almost identical, we expect that for both species the rotational principal axes and the rotational diffusion time scales to be very similar. Since the acetate orientation will be random with respect to the photoacid optical transition moment from the beginning of the time-dependent reaction, we do not have to include any anisotropy dependencies into the interpretation of the acetic acid marker mode.

The polarization-dependent UV-pump IR-probe signals as function of pulse delay t are then fully described by

$$S_{par}(t)=\tfrac{1}{3}S(t)[1+2r(t)], \tag{37}$$

$$S_{par}(t)=\tfrac{1}{3}S(t)[1-r(t)], \tag{38}$$

with $S_{par}(t)$ the pump-probe signal for parallel polarization configuration and $S_{per}(t)$ for perpendicular polarization of the UV-pump and IR-probe pulses.

III. EXPERIMENTAL METHODS

We used femtosecond mid-infrared (mid-IR) spectroscopy after reaction initiation with an optical trigger pulse to follow specific infrared active vibrational marker modes, present at the proton-donor (either in photoacid or photobase form) and proton-acceptor sides (indicating the conjugate acid of acetate, acetic acid). The second harmonic of a home-built 1 kHz amplified Ti:sapphire laser system (wavelength 400 nm, pulse duration 55 fs, energy 3–7 μJ, spot diameter 200 μm) was used to excite a 100 μm thick jet of the sample solutions. Tunable mid-infrared probe pulses of 100–150 fs duration were generated by difference frequency mixing of signal and idler pulses from a near-infrared optical parametric amplifier.[100] After spectral dispersion with a polychromator the probe pulses were detected by a multichannel detector for the mid-IR.

The technique used to acquire fluorescence decay signals was time-correlated single-photon counting, using a Ti:sapphire laser (Tsunami pumped by a Millenia X, both purchased from Spectra-Physics) operated at 82 MHz, 1 ps pulses, wavelength 400 nm). The photocounting data were recorded at 3.14 ps/channel with instrument response function having a full width at half maximum of 20–23 ps.[101]

UV-visible absorption measurements were performed using a Hewlett-Packard 8452A diode array spectrophotometer with the spectral resolution of the measurements of 0.2 nm. The steady-state fluorescence experiments were carried out on a SLM-AMINCO-Bowman2 spectrophotometer. Typically, five to nine measurements were taken and averaged for

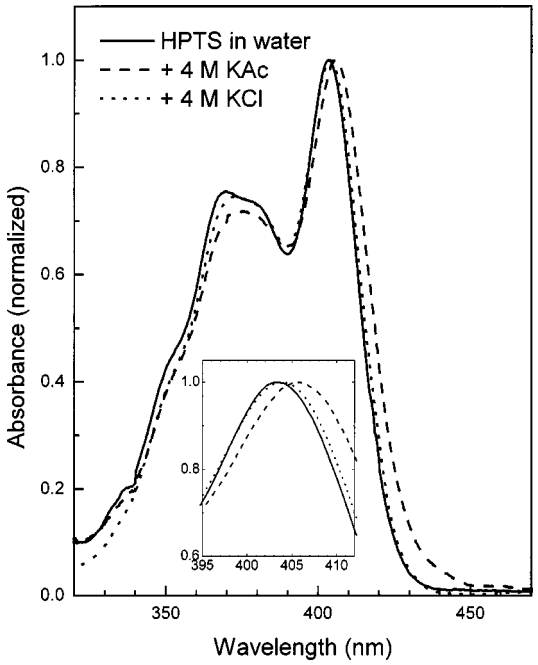

FIG. 3. The absorption spectra of HPTS in water and in aqueous solutions of $4M$ KAc and $4M$ KCl.

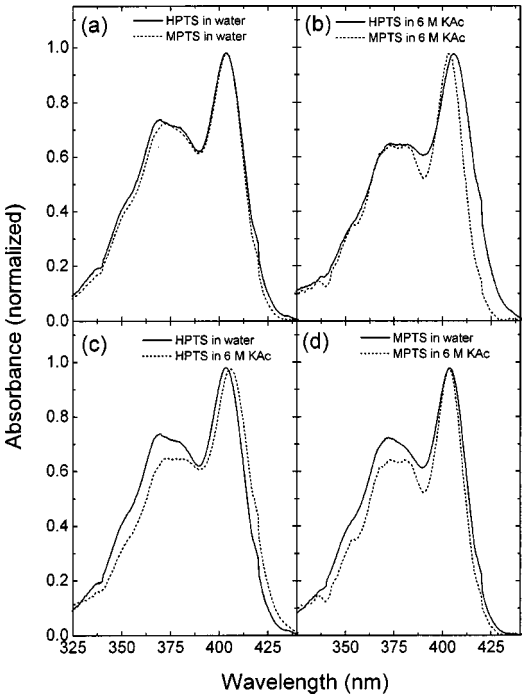

FIG. 4. UV-VIS absorption spectra of HPTS and MPTS measured in water and in $6M$ aqueous solution of potassium acetate.

each spectrum. The blank recording was then subtracted from the averaged spectra and the resulting spectra were corrected.

We used 20 mM solutions of HPTS (8-hydroxy-1,3,6-trisulfonate-pyrene, Aldrich) in deuteriumoxide (Deutero GmbH, 99.8% deuteration grade). Potassium acetate (Aldrich) was used in the studies as the proton acceptor base in the concentration range of $[(0.25-4)M]$. A small amount of deuterated acetic acid (CH_3COOD, Aldrich) was added to ensure that HPTS was present in the ground state in the acid form. (Since we use small amounts of acetic acid, less than $0.05M$ H-contamination does not occur, as confirmed in additional check experiments.) The methoxy derivatives of HPTS, MPTS (8-methoxy-1,3,6-trisulfonate-pyrene, Aldrich), was used as a control in steady-state measurements.

All measurements were performed at room temperature, $T=25\pm2$ °C.

IV. RESULTS AND DISCUSSION

A. Steady-state UV-VIS spectra

We have conducted steady-state UV-VIS spectral measurements of HPTS in solutions containing potassium acetate in concentrations up to $9M$. We have observed a red shift of 1.3 nm, 2.6 nm, 3.5 nm, and 4 nm in the electronic absorption spectra of HPTS at $1M$, $4M$, $6M$, and $9M$ of potassium acetate, respectively, showing a saturation effect as expected when assuming direct complexation reaction between the base and the photoacid in the electronic ground state. In comparison, the absorption spectra of HPTS taken in $4M$ KCl in H_2O (limit of solubility of KCl is $4.15M$ at 25 °C) has yielded a much smaller red shift in the absorption spectra of ~0.5 nm (Fig. 3).

We have also measured as an alternative check the absorption spectra of the methoxy derivative of HPTS (MPTS) in the same set of solutions. In MPTS the hydroxy group is replaced with a methoxy group, so MPTS cannot form hydrogen-bonding complexes with acetate. Figure 4 compares between HPTS and MPTS and shows the practically negligible spectral shift when adding $6M$ acetate to a solution of MPTS. We have observed by the same spectral method the complexation of HPTS with the formate base in water, so the complexation with the acetate base was not found to be unique. To verify whether a 1:1 complexation between HPTS and the acetate base occurs, we fitted each absorption spectrum of HPTS in potassium acetate solution as being made of two spectra with varying relative weights: one was the spectrum of HPTS in pure water, and the other the absorption spectrum of HPTS in $9M$ solution of potassium acetate where full complexation was assumed in the ground state of HPTS. All absorption spectra of HPTS up to $9M$ of acetate concentration were fully reconstructed with no additional fitting parameters. Figure 5 shows a representative reconstruction of the HPTS absorption spectrum in $3.4M$ solution of potassium acetate in which case the two forms of HPTS, complexed and uncomplexed, were found to be in roughly equal amounts.

The relative contributions of the two species of HPTS found as function of the acetate concentration up to $9M$ acetate are subject to a 1:1 complexation process between HPTS and acetate with a complexation constant $K_{HB}=0.28M^{-1}$ (Fig. 6).

We have also extracted the complexation constant by comparing the amplitude of the initial component relative to the total acetic acid signal in the IR-time-resolved measurements. The following relative fractions of HPTS directly

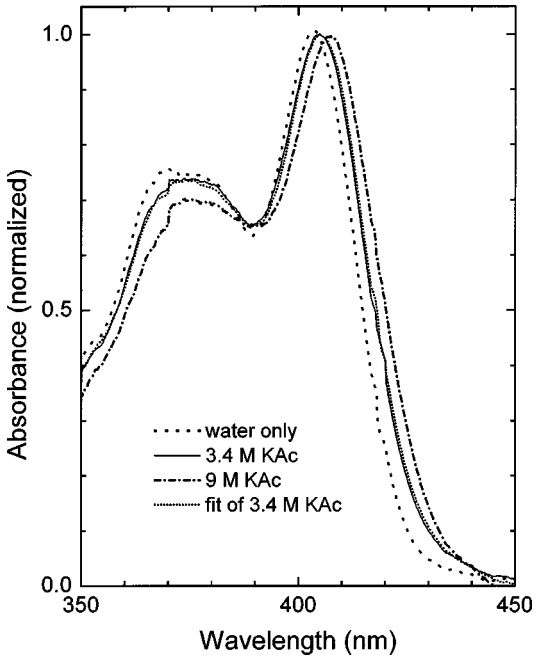

FIG. 5. The fitted spectrum of the absorption spectra of HPTS in 3.4*M* KAc by linear combination of two weighted absorption spectra of HPTS in water and in 9*M* KAc with weighting coefficients of 0.56 and 0.46, respectively.

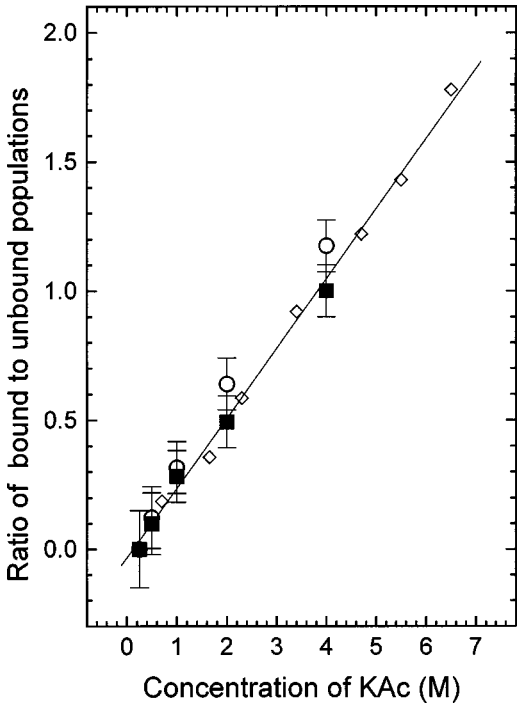

FIG. 6. Ratio of hydrogen-bonded to unbonded populations vs concentration of KAc. Diamonds: from the absorption spectra of HPTS, $K=0.28M$. Circles: from the initial amplitudes of the time-resolved IR measurements (Ref. 87), $K=0.3M^{-1}$. Squares: from the initial amplitudes of the time-resolved IR measurements, this work (Table I), $K=0.26M^{-1}$. The slope of the fitting line is equal to the complexation constant for the steady-state measurements.

complexed to acetate have been deduced: 0.54 in $4M$, 0.39 in $2M$, 0.24 in $1M$, and 0.11 in $0.5M$ solutions of potassium acetate; no detectable initial fraction was observed in $0.25M$ acetate.[88] We obtain from this analysis a complexation constant of $0.3M^{-1}$, which is practically identical to the complexation constant derived from the analysis of the optical spectral shift in the absorption spectra of HPTS.

The equilibrium constant found for the complexation process between HPTS and acetate corresponds to a free energy of complex formation of about 0.7 kcal/mol. Interestingly, recent calculation of the free energy of formation of the hydrogen bonding complex between the acetate base and phenol in pure water resulted with the value of 3.6 kcal/mol. For the less-polar solvent dimethylsulfoxide (DMSO) the corresponding value was calculated to be 1.3 kcal/mol.[102] The calculations were made for the formation of the 1:1 hydrogen bonding complex between phenol and acetate with a similar configuration to the one depicted in Fig. 2. Although this theoretical study may serve as a support for our assignment of the complexation constant between HPTS and acetate to the formation of the directly linked acid-base complex with no water molecules in between acid and base, one should keep in mind the important differences between HPTS-acetate and phenol-acetate systems. HPTS is a much stronger ground-state acid than phenol ($pK_{\mathrm{HPTS}}\approx 7$ at $1M$ acetate while $pK_{\mathrm{ph}}\approx 9.9$ in pure water). In addition, the complexation constant of HPTS was measured in concentrated strong electrolyte solution for which a considerable change in the thermodynamic properties may occur compared those in the pure solvent environment. Finally, HPTS is triply charged, whereas phenol is a neutral molecule, which may affect the extent of the interaction with the negatively charged acetate ion. However, at above $1M$ concentration of a strong electrolyte we expect the charge of HPTS to be effectively screened and its interaction to resemble the interaction of a neutral photoacid.[72]

In passing, we note that the complexation constant between phenol and acetate in water is expected to be much larger in less polar aprotic solvents such as DMSO and acetonitrile. This has indeed been verified experimentally[103,104] in acetonitrile, where a complexation constant of about 660 was measured for the phenol-acetate hydrogen-bonding complex. When comparing with almost any other solvent, it is much more difficult to create stable hydrogen-bonding complexes in water. In fact, in water a direct hydrogen bond between a complexing base and an acid must replace at least two existing hydrogen bonds which the acid and base each form separately with the solvent, thus making direct complexation between the acid and base typically an unfavorable process in dilute aqueous solutions. Only in the case of highly concentrated aqueous solutions of carboxylic bases it is possible to form direct hydrogen-bonding complexes between the photoacid and the base.[72,88]

B. Transient IR spectra of HPTS in D_2O

In our previous report[88] we have indicated that the most significant changes between the IR spectra of electronic ground-state photoacid and photobase occur in the 1250–1600 cm^{-1} frequency range, where vibrational bands of modes with aromatic ring and/or C-O stretching activity are found (whereas bands between 950 and 1250 cm^{-1} are asso-

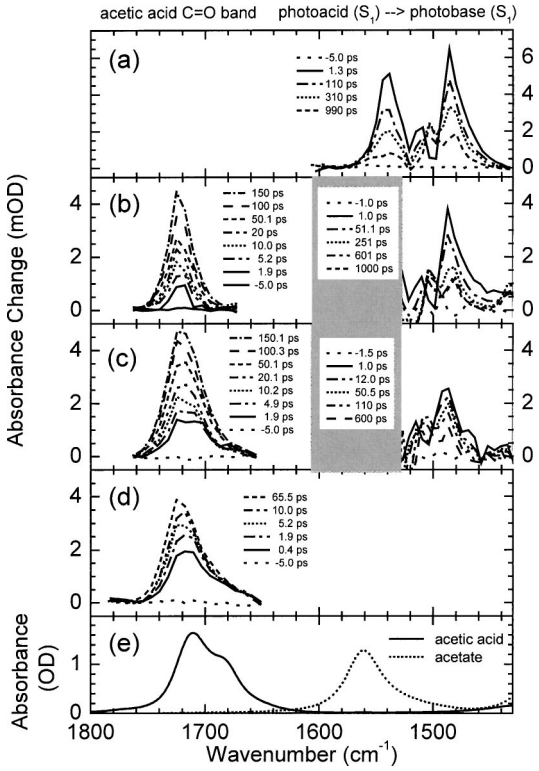

FIG. 7. Transient spectra of HPTS acid and base forms (1350–1600 cm^{-1}) are shown in panel (a) in D_2O (no acetate), and in 0.5M (b) and 1M (c) solution of acetate; note the opaque region due to steady-state absorption of acetate between 1650 and 1520 cm^{-1} for cases (b) and (c). The transient increase of acetic acid signal is shown for 0.5M (b), 1M (c), and 4M (d) solutions of acetate (1650–1780 cm^{-1}). The steady-state IR spectra of acetic acid and acetate anion in D_2O are depicted in panel (e).

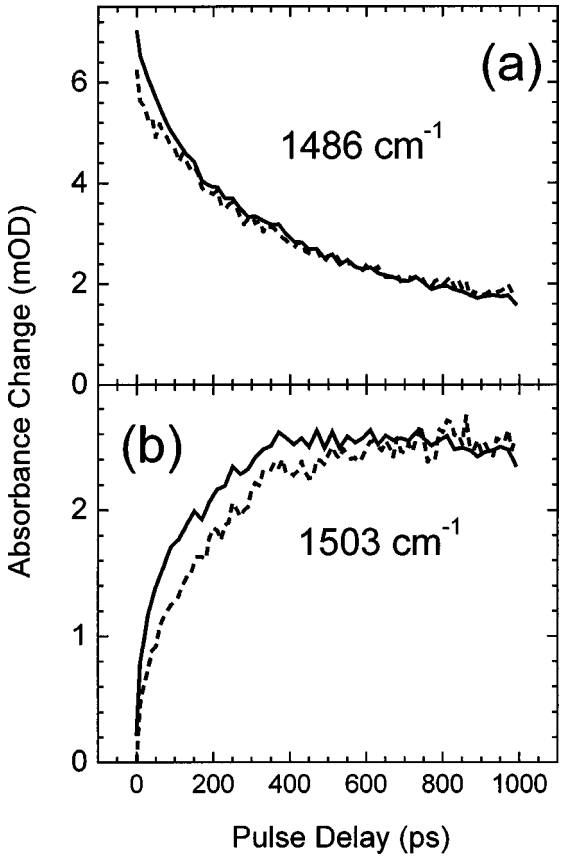

FIG. 8. Transient band intensities of HPTS in D_2O showing the influence of the rotational anisotropy decay on the photoacid (1486 cm^{-1}) and conjugate photobase (1503 cm^{-1}) bands. Solid lines denote the response for parallel polarization direction of UV-pump and IR-probe pulses, dashed lines indicate the perpendicular configuration.

ciated with motions of the SO_3^- groups). Indeed, substantial absorbance changes occur in the same upper part of the fingerprint region for the photoacid and photobase in the electronic excited state (see Fig. 7).

We allocate[88] a transient band at 1486 cm^{-1}, which appears upon electronic excitation of HPTS within time resolution, to be indicative of the photoacid in the S_1 state, and a band at 1503 cm^{-1}, which grows in on a time scale of several hundreds of picoseconds in the case of HPTS in D_2O (no acetate added), to be a marker for the deuteron transferred HPTS (photobase) in the S_1 state. The photoacid band at 1486 cm^{-1} is replaced by a photobase band at the same frequency with a weaker transition moment, indicating that the transition is likely to be due to the same vibrational mode. We refrain from analyzing the signals more thoroughly because of the overlap of the bands for the photoacid and photobase S_1 states. We have measured the signals at parallel and perpendicular polarizations to correct for rotational anisotropy decay (Fig. 8). Analysis of the data shown in Fig. 8 using Eqs. (36)–(38) leads to the finding that the infrared transition dipole moment of the HPTS photoacid band at 1486 cm^{-1}, with its almost identical dynamical behavior for parallel and perpendicular polarization configurations, is about 50° tilted from the optical excitation transition dipole moment, i.e., very close to the magic angle. On the other hand the transition dipole moment of the photobase band at 1503 cm^{-1} is closer aligned in the direction of the optical transition dipole moment of the photoacid electronic excitation (angle 30–35°). The time constant for anisotropy decay is about 150 ± 30 ps, assuming spherical rotational diffusion. The deuteron transfer has been found to occur with a 250 ps time constant ($T = 25 \pm 2$ °C), in accordance with previous reports.[105]

We have studied the deuteron transfer dynamics of HPTS to acetate as a function of acetate concentration in the range of (0.25–4)M of acetate. By probing these photoacid and photobase IR marker modes we are able to observe when the deuteron leaves the photoacid. We have inspected the dynamics of the IR active C═O stretching mode of acetic acid located at 1720 cm^{-1} to monitor when the deuteron arrives at the accepting base (Fig. 7). Detection of the rise of the latter acetic acid absorption band serves as a direct measure for the fraction of acetic acid generated by deuteron transfer, since no other species (HPTS photoacid and photobase or the acetate base) contributes in this frequency range. In the case of the photoacid and photobase bands around 1500 cm^{-1}, overlap of absorption bands does occur. We have used singular value decomposition to extract the dynamics of these bands.

As already been reported by us,[88] the deuteron transfer reaction as reflected by the transient appearance of the acetic acid band was found to be bimodal. For acetate concentrations between 0.5M and 4M, an initial population of the

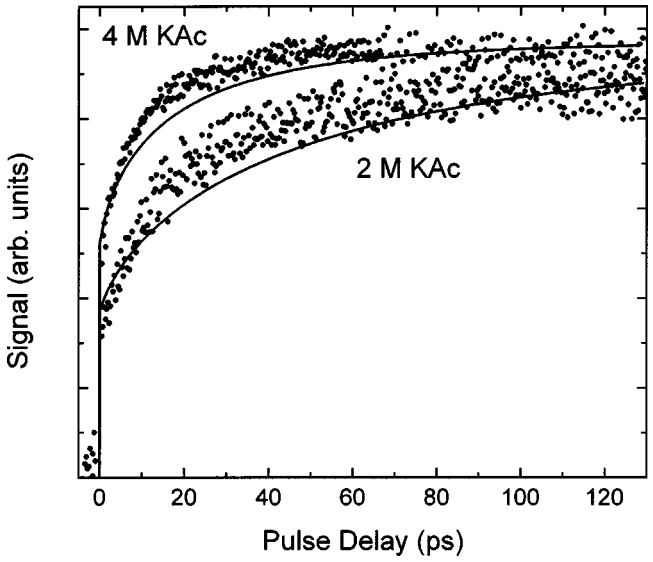

FIG. 9. Transient experimental band intensities of the acetic acid for specific acetate concentration (dots, triangles). Solid lines are calculated curves with the instrument-limited rise components of 0.54 in $4M$ and 0.39 in $2M$ using the SCK model, Eqs. (25a) and (27). The parameters used in the fit are summarized in Table I.

acetic acid (the amplitude depends on the acetate concentration) appears within time resolution of 150 fs, to be followed by an additional, much slower, rise of the acetic acid signal that at long times follows the diffusion-encounter reaction model. We have previously analyzed this part of the proton-transfer reaction using the SCK model assuming fully screened potential [$U(r)=0$, Eq. (26)].[88] The rationale behind this analysis was the very high concentration of strong electrolyte present in the solutions of the photoacid. The value of $1/\kappa_{\mathrm{DH}}=1.5$ Å calculated for the screening length at $4M$ acetate is so small that the effect of the potential is altogether marginal at such high concentrations. Clearly, the importance of the potential increases with the decrease in the electrolyte concentration. In the present report we have studied solutions down to $0.25M$ of electrolyte, and thus we have decided to use the DH ionic screening potential throughout the concentration range down up to $4M$ of acetate in order to keep the analysis consistent for all concentrations.

We have found the amplitude of the initial fast rise of the acetic acid signal to be concentration dependent. Figure 9 shows the bimodal rise of the experimental acetic acid signal in D_2O solutions containing $2M$ and $4M$ of acetate base. Figure 9 also shows data fits using the SCK-Szabo model with screened Coulomb potential, Eqs. (25a) and (27), using the DH ionic screening law, Eqs. (28)–(30).

The values for the physical parameters necessary for the kinetic calculations using the SCK-Szabo model have been taken from previous studies[95,105] and have been assumed to be fixed reaction parameters for each given solution of HPTS and acetate (Table I). The following values of the diffusion coefficient have been used to account for the change in the solution viscosity at different concentrations of potassium acetate, $D=(0.6–1.3)\times10^{-9}\ \mathrm{m^2\ s^{-1}}$. We have used the literature values of $a=6.3$ Å and $R_D=21.3$ Å (Refs. 95 and 105) for the contact separation and the Debye radius, Eq. (30), for the direct proton-transfer reaction between HPTS and acetate, respectively. Taking into account the ionic screening effect, we have obtained values for $1/\kappa_{\mathrm{DH}}=6–1.5$ Å, and of $a_{\mathrm{eff}}=3.3–5.7$ Å for the acetate concentration range of $(0.25–4.0)M$.

Figure 9 shows that the data fits using the SCK model for the diffusive part of the deuteron transfer reaction do not reproduce accurately the observed kinetics of the rise of the acetic acid signal at high acetate concentrations. The quality of the data is considerably improved by adding a static reaction component to the SCK model, Fig. 10. The implication of this observation will be discussed below in the following section.

For the lower concentration range of acetate, also shown in Figs. 10 and 11, we have observed, as considered in Refs. 96 and 97, an increasing influence of the indirect deuteron transfer mechanism where the photoacid first dissociates to the solvent and then the deuteron is picked up by the acetate base in a diffusion controlled reaction, Eqs. (31)–(35). To account for the scavenging process, the following reaction parameters were used for the direct acetate-deuteron reaction $D'=(5.4–6.8)\times10^{-9}\ \mathrm{m^2\ s^{-1}}$, $a'=5.5$ Å, $R'_D=7.1$ Å, and effective reaction radius $a'_{\mathrm{eff}}=(6.7–6.1)$ Å for the acetate concentration range of $(0.25–1.0)M$, see Table I and Refs. 73, 96, and 97.

The fits to the experimental data have been optimized by a global run over the full range of acetate concentrations [$(0.25–4)M$]. Figure 9 portrays data fits using a uniform value for the intrinsic SCK rate constant at contact for all acetate concentrations, $k_0=(12.5\pm1\ \mathrm{ps})^{-1}M^{-1}=(8\pm1)\times10^{10}M^{-1}\ \mathrm{s^{-1}}$. Using this value for k_0, the initial pseudo-first-order rate constant at contact, $c_0k_0e^{-\beta U(a)}$, has been found to be $(6\ \mathrm{ps})^{-1}$ and $(14\ \mathrm{ps})^{-1}$ at $4M$ and $2M$ of acetate, respectively, in a similar range of the values of $(7.5\ \mathrm{ps})^{-1}$ and $(15\ \mathrm{ps})^{-1}$ found by assuming full screening.[88]

TABLE I. Parameters of the fits of the short delay scans up to 150 ps.

$c\,[M]$	Amplitude (Tight complex)	Amplitude [$\exp(-t/6\ \mathrm{ps})$]	a_{eff} (Å)	a'_{eff} (Å)	[a]D ($10^{-9}\ \mathrm{m^2\ s^{-1}}$)	[b]D' ($10^{-9}\ \mathrm{m^2\ s^{-1}}$)	k_w ($\mathrm{s^{-1}}$)	k_0 ($M^{-1}\ \mathrm{s^{-1}}$)
4	0.5	0.25	5.7		0.6			
2	0.33	0.15	5.2		0.9			$(8\pm1)\times10^{10}$
1	0.22	0.07	4.7	6.1	1.1	5.4	2.9×10^9	
0.5	0.09	0.05	4.0	6.4	1.2	6.5	3.3×10^9	

[a]$D=D_{\mathrm{Ac^-}}+D_{\mathrm{HPTS}}$.
[b]$D'=D_{\mathrm{Ac^-}}+D_{\mathrm{D^+}}$.

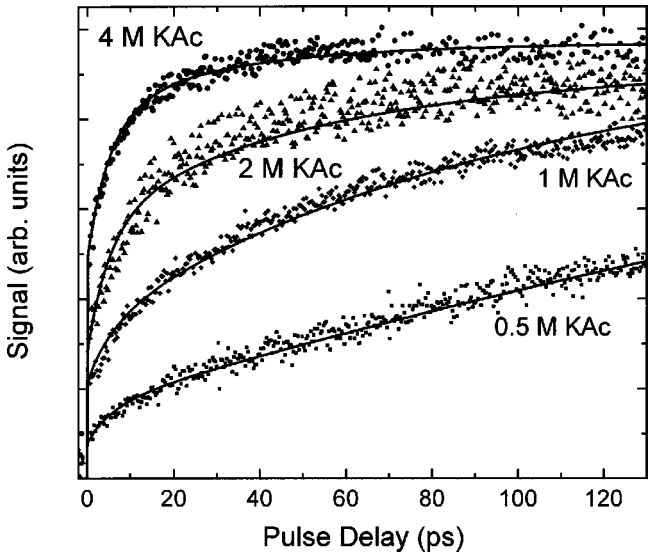

FIG. 10. Transient experimental band intensities of the acetic acid for specific acetate concentration (dots). Solid lines are calculated curves with static components and diffusive part according to Eq. (25a) with the parameters summarized in Table I.

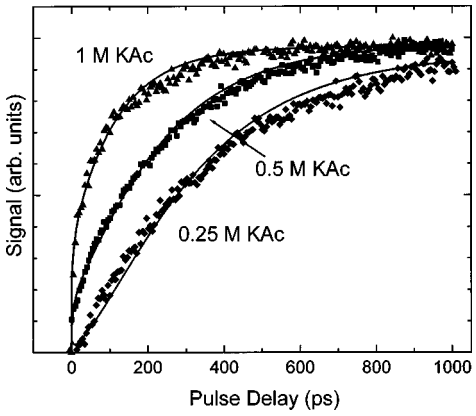

FIG. 11. The rise of the acetic acid taken over an extended period of time. Solid lines are calculated curves using Eq. (35) with parameters summarized in Table II.

With addition of a static reaction component to the SCK model we achieve a substantial improvement of the fits at $4M$ and $2M$ of acetate (Fig. 10); the χ^2 value of the $4M$ fits decreases from 16 to 3.4. The following relative amplitudes of the static reaction rate component of 6 ps duration have been used in the data fits: 0.25 in $4M$, 0.15 in $2M$, 0.07 in $1M$, 0.05 in $0.5M$, and 0.03 in $0.25M$. We attribute this static component in the diffusion influenced deuteron transfer reaction to the fraction of weakly interacting pairs already at close range to (but not directly complexed to) each other at the time of the initiation of the reaction, so the subsequent reaction will be not delayed by diffusion. The reaction rate of this fraction of molecules is directly related to the unimolecular recombination rate constant of the acid-base complex, k_r, of the Eigen-Weller model and can be identified with k_r if one assumes that it represents the unimolecular reaction rate of acid-base encounter pairs separated by the contact distance a. The validation of the correspondence between k_0 and k_r has been sought for long time in proton-transfer reactions where contact recombination has been for long considered an excellent assumption, as opposed to electron and energy transfer reactions where reactive pairs interact over relatively long distances with reaction rates that are distance dependent. The assignment is self-consistent with the data fits of the diffusive part of the proton-transfer reaction which have yielded an intrinsic SCK rate constant of $k_0 = 8 \times 10^{10} M^{-1}\,\mathrm{s}^{-1}$. By Eq. (20) we find for the proton-transfer rate of the acid-base complex at contact separation, k_r, $k_r = 1.6M \times k_0 = 1.3 \times 10^{11}\,\mathrm{s}^{-1}$ which translates to a static (exponential) component of about 7 ps independent of the bulk concentrations of the acid and base. This value agrees well with the 6 ps (exponential) component that we have found in the rise kinetics of the acetic acid signal (Fig. 10).

C. The long time reaction regime and the approach to steady-state diffusion-assisted reaction kinetics

The most important phase in acid-base reactions at low concentrations is the relatively long time regime where the bulk of the reaction is carried out with a steady-state rate constant. In the present study we have investigated both the very short and the long time regimes of the acid- base reaction between HPTS and acetate. Since the long time regime is also accessible to optical probing it is important to verify that the transient IR measurements at long times matches with the high-sensitivity single-photon-counting measurements taken at similar experiment conditions. We have thus extended the time scale of the transient IR measurement to 1 ns for the low and intermediate concentrations of acetate $[(0.25-1)M]$. We have first compared measurements of the rise of the C═O band of acetic acid at 1720 cm^{-1} (Fig. 11) with the rise of the HPTS-photobase IR band at 1503 cm^{-1} (Fig. 12). The kinetics are shown in Fig. 12 after correction for the fluorescence lifetime and for rotational anisotropy effects on the photobase band.

For concentrations of $1M$ of acetate comparison of the rise times of the photobase and the acetic acid signals shows that direct deuteron scavenging by the base dominates the deuteron transfer dynamics, and as such both transients can adequately be described by Eq. (25a) using an identical value set of reaction parameters. As a result, we can safely assume that for higher concentrations of base the direct scavenging mechanism dominates (we cannot measure the photobase 1503 cm^{-1} band at higher concentrations because the solutions become opaque at this frequency due to a nearby steady-state band of acetate.) In contrast, for lower concentrations of acetate we have observed that the photobase signal, as described by Eq. (23), rises with faster rate than the acetic acid signal, as described by Eq. (35). This observation indicates an increasing importance of the indirect deuteron transfer mechanism at lower base concentrations, where the photoacid first dissociates to the solvent after which the deuteron is picked up by the acetate base in a diffusion controlled reaction.

The calculated kinetic responses appear to mimic the

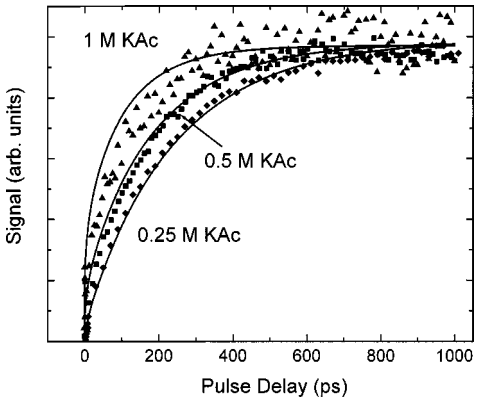

FIG. 12. The rise of the photobase signal corrected for rotation and the excited state lifetime. Solid lines are calculated curves according to Eqs. (23) and (27) with the parameters summarized in Table II.

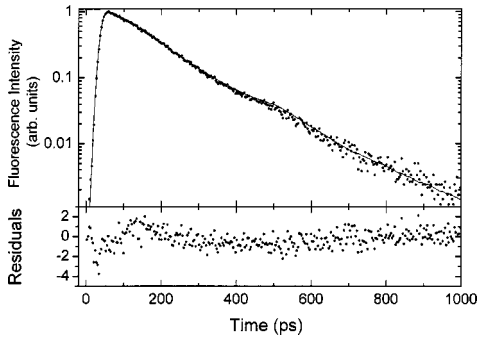

FIG. 13. TCSPC decay of the HPTS photoacid measured in 1*M* acetate base solution in D_2O (squares) on a logarithmic scale. The data are fitted by convoluting decaying exponent (τ=105 ps) with the instrument response function (dots) $\chi^2=0.81$.

observed time-dependent signals for both HPTS-photobase and acetic acid bands in a consistent way (Figs. 11 and 12). The analysis of the relatively slow kinetics of the deuteron transfer below 1*M* has—with considerable confidence—resulted with an estimation of the intrinsic deuteron transfer rate of $k_0=(9\pm1)\times10^{10}M^{-1}\,s^{-1}$, within uncertainty range equal to the directly determined rate constant derived from fitting the results obtained on solutions with above 1*M* acetate concentrations. We conclude from this that transient IR spectroscopy is a reliable measurement technique for chemical reaction dynamics from about 150 fs to 1 ns, a time range of about four orders of magnitude. The 1 ns time scale is easily accessible to high-resolution time correlated single-photon counting techniques (TCSPC techniques). We have collected the time resolved fluorescence of the photoacid at 420 nm, detuned from the fluorescence peak of the photoacid to avoid the small overlap with the fluorescence of the photobase. The time-resolved data have been recorded with an instrument response function (IRF) of about 20 ps. Figure 13 shows the time-resolved emission of HPTS in D_2O at a concentration of 1*M* of acetate. As reported previously by Pines *et al.* on measurements carried out in H_2O,[72] the measured decay of the photoacid is reasonably described by one decaying exponent with a pseudo-first-order rate constant $k'=(105\,ps)^{-1}$ after IRF deconvolution (Fig. 13). A double exponential fit would improve the quality of the fit by about 10% (where the second component has 7% of total amplitude and 20% faster decay than first component). This is because the partial masking of the acid-base dynamics by the parallel proton-transfer-to-solvent reaction of the photoacid and the effective diminishing of the geminate recombination reaction between the HPTS anion and the proton (deuteron) due to the very efficient proton (deuteron) scavenging by the acetate base and to almost complete ionic screening.[96,97] To show that this apparent near-exponential decay of the TCSPC signal is consistent with the multiphase dynamics found in our femtosecond-time-resolved IR measurements, we used Eq. (22) with kinetic parameters found by the IR measurements to generate the full survival probability of the excited HPTS, $S_{ROH}(t)$ (assuming that under these reaction conditions deuteron geminate recombination does not contribute to the decay function of the photoacid, a fairly correct assumption[73,96,97]) and convoluted it with the IRF of the TCSPC system.

The resulting fit between the measured (points) and simulated (solid line) signals is shown in Fig. 14. The overall accuracy of the fit remains impressive even when the experimental data are shown on a logarithmic scale covering more than three decades of signal amplitude. The bimodal nature of the reaction is completely masked by the limited time resolution of the TCSPC experiment. Moreover, since in this experiment $k(t)$ becomes practically equal to k_{SCK}^{SS} after about 50 ps $S_{OH}(t)$ decays in exponential fashion from about 50 ps onwards with a pseudo-first-order rate constant equal to $k_W+c_0k_{SCK}^{SS}=(350\,ps)^{-1}+(152\,ps)^{-1}=(105\,ps)^{-1}$, where k_w is the deuteron transfer rate from HPTS to D_2O in presence of 1*M* potassium acetate, k_{SCK}^{SS} is the steady-state SCK reaction rate constant between acetate and HPTS, Eq. (12), and $c_0=1M$. We conclude that at long times our measured IR signal is practically identical to the measured optical decay of the photoacid by the TCSPC technique.[72] It should also be clear that the magnitude of k_r could only be roughly estimated at very high acetate concentrations by the TCSPC technique due to limited time resolution.[72] On the other hand, the very high dynamic range

TABLE II. Parameters of the fits of the long delay scans up to 1000 ps.

$c\,[M]$	Amplitude (Tight complex)	Amplitude $[\exp(-t/6\,ps)]$	a_{eff} (Å)	a'_{eff} (Å)	D ($10^{-9}\,m^2\,s^{-1}$)	D' ($10^{-9}\,m^2\,s^{-1}$)	k_w (s^{-1})	k_0 ($M^{-1}\,s^{-1}$)
1	0.22	0.07	4.7	6.1	1.1	5.4	2.9×10^9	
0.5	0.09	0.05	4.0	6.4	1.2	6.5	3.3×10^9	$(9\pm1)\times10^{10}$
0.25	0	0–0.03[a]	3.3	6.7	1.3	6.8	3.7×10^9	

[a]No apparent change in the accuracy of the data fit in this amplitude range.

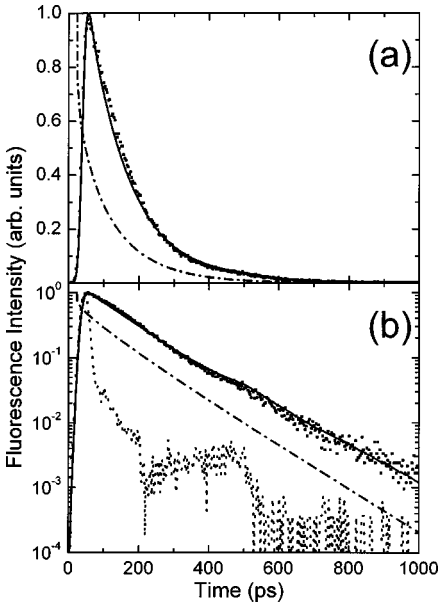

FIG. 14. TCSPC decay of the HPTS photoacid measured in 1*M* acetate base solution in D_2O (squares) shown on a linear (a) and on a logarithmic (b) scale. Dashed and dot line is calculated decay using Eqs. (22) and (27), solid line is the convolution of Eq. (23) with the instrument response function (dots). The reaction parameters used in the calculation are taken from the analysis of the time-resolved IR experiment, $\chi^2=2.9$.

of the TCSPC signal does allow the detection of nonexponentiality in the diffusive part of the decay signal of the photoacid such as reported by Cohen *et al.* for the 2-naphthol-6-sulfonate reaction with sodium acetate in water/glycerol solutions.[74,75] We conclude the discussion in this section by stating that we demonstrate in the current work that time-resolved IR measurements are a powerful experimental approach for monitoring diffusion influenced reactions from the earliest onset on a time scale of 150 fs to long reaction times up to 1 ns, when the reactions assume steady-state behavior. We expect that time-resolved infrared spectroscopy will become a powerful tool for monitoring the reaction progress in a broad range of chemical reactive systems.

V. THREE-STAGE REACTION MECHANISM FOR GENERAL ACID-BASE REACTION

The model of acid-base reactions in aqueous solutions, which emerges from our observations, indicate a more complex reaction scheme than what was traditionally envisioned by the Eigen-Weller model. We have identified bimodal behavior not considered by this traditional EW model. Bell indicated in 1980 that a three-stage proton-transfer scheme is consistent with Marcus treatment of proton transfer.[89] Indeed, in view of our recent observations the traditional proton-transfer rate on contact (k_r in the EW context) must be regarded as an outer sphere (overall) rate constant. In our experiments the actual on-contact (intrinsic) rate constant has been found to be at least two orders of magnitude faster. A possible way to take into account these observations is by extending the EW model from a two-stage to a three-stage reaction scheme as was considered by Bell.[89] In the first

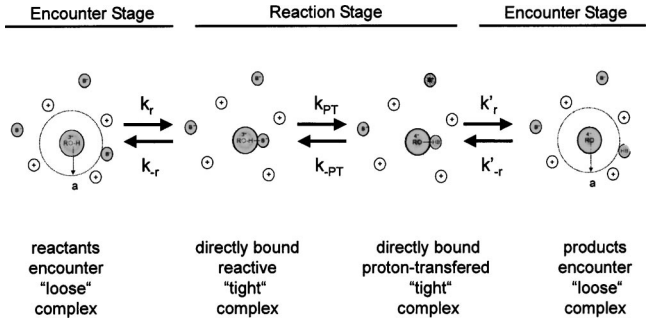

FIG. 15. Proposed refined Eigen-Weller model with a three-stage mechanism consisting of diffusion, encounter, and reaction stages. The Eigen-Weller ''on-contact'' reaction rate k_r is to be understood as a rate for solvent shell reorganization during which the loose encounter complex reforms to a directly bound reactive tight complex, which promptly transfer a proton along the reaction coordinate with rate k_{PT}.

stage of the reaction, the acid and base form a ''loose'' encounter complex each retaining its water solvation shell. This stage is governed by diffusion and the encounter complex is described by the contact distance *a*. The second stage of the reaction occurs within the contact volume and is largely controlled by the solvent. We propose that the time scale for the second reaction stage is due to a possible small activation barrier and to—more importantly—solvent reorganization dynamics. The observed time constant of 6 ps is slightly faster than the Debye relaxation time of water (which is about 10 ps), but still slower than the longitudinal relaxation time τ_L (which has a value of about 0.5 ps). This intermediate reaction stage is relatively slow compared to the final, inner sphere reaction stage of the proton transfer which we have found to be faster than 150 fs.

We thus propose the following three-stage proton-transfer reaction scheme outlined below as a possible general mechanism for proton transfer in acid-base reactions in aqueous solutions (Scheme 2, Fig. 15):

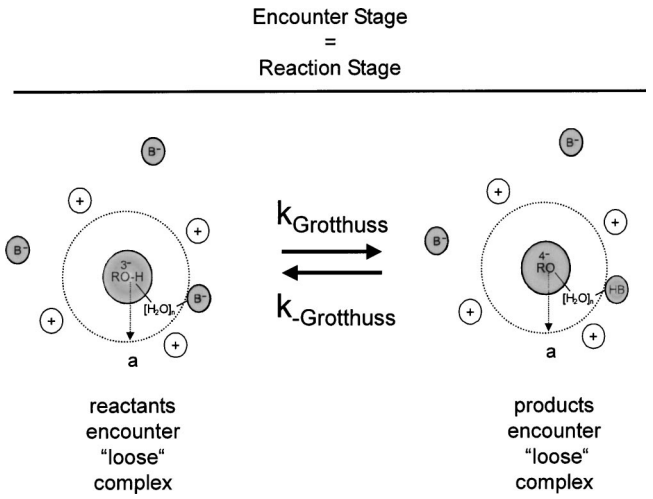

FIG. 16. Alternative explanation for the slower on-contact reaction rate k_r found for the loose encounter complex. Here the proton transfer proceeds along a water network (water wire) through a von Grotthuss mechanism, with $k_{\text{Grotthuss}}=k_r$.

Diffusion stage		Encounter stage		Reaction stage
ROH+B	$\underset{k_{-D}}{\overset{k_D}{\rightleftarrows}}$	$(\mathrm{ROD}\cdots(\mathrm{D_2O})_n\cdots\mathrm{B})_{\mathrm{loose}}$	$\underset{k_d}{\overset{k_r}{\rightleftarrows}}$	$(\mathrm{RO-D}\cdots\mathrm{B})_{\mathrm{tight}}\underset{k_{.pt}}{\overset{k_{pt}}{\rightleftarrows}}(\mathrm{RO}\cdots\mathrm{D-B})_{\mathrm{tight}}$

Scheme2

Here loose and tight complexes indicate the solvent separated and directly linked acid-base complexes. The steady-state rate constant of a three-stage reaction model is straightforward:[92]

$$k_f=\frac{k_{PT}k_Dk_r}{k_dk_{-D}+k_{PT}(k_r+k_{-D})}. \tag{39}$$

According to our findings k_{PT} is likely to be much larger than all other rate constants when the proton transfer reaction is exothermic, $k_{PT}\gg k_D$, k_r-k_{-D}, making

$$k_f\approx\frac{k_Dk_r}{k_r+k_{-D}}, \tag{40}$$

which is the observable reaction rate identical to the overall two-stage reaction rate constant of Eigen and Weller, Eq. (1). As discussed before, k_r is related to k_0 according to

$$k_r=\frac{k_0}{\frac{4\pi a^3}{3}N}, \tag{20'}$$

and is usually assumed to be larger than the rate constant for the separation of the reactant by diffusion, k_{-D}. This allows to make an additional approximation which is most commonly used for the favorable direction of a reversible acid-base reaction, $k_f=k_D$. In our experiment we have found $k_r=(6\ \mathrm{ps})^{-1}$, which within our experimental conditions of concentrated electrolyte solutions is in line with this assumption. We note that at infinite dilution k_{-D} of the HPTS-acetate system is extremely large $[(3\ \mathrm{ps})^{-1}]$ due to the large Coulomb repulsion between the negatively charged HPTS and the acetate anion. In this case $k_{-D}>k_r$ and the overall proton-transfer rate is expected to be considerably smaller than the diffusion-controlled rate although the proton-transfer reaction is exothermic.

As we already discussed in great detail, we have found the proton transfer that tight complexes of the photoacid and the acetate base occurs in within 150 fs. One can consider the kinetics of such ultrafast acid-base reactions to take place in three different concentration regimes. When k_0 (and k_r) are large compared to diffusion, reaction rates measured at low concentrations will only reveal the diffusion-limited rate constant k_D. Raising the concentration to intermediate values can potentially reveal the encounter stage reaction rate between the acid and base, k_0 and k_r. Measurements in this concentration range will potentially result in estimation of time-dependent rate constants.[73–75] Using the SCK reaction model one would determine the value of the bimolecular encounter stage rate constant k_0 or, alternatively, using the EW model, the through-solvent unimolecular rate constant k_r. Raising the concentration even further may result in the formation of tight acid-base complexes through hydrogen-bonding interactions.[106] Experiments in this concentration range may thus result in the measurement of the most inner proton-transfer rate constant.[88] This three-stage reaction scheme is consistent with the observation of Eigen and Weller of the large contact distance found in many diffusion-controlled acid-base reactions. For example, the self-neutralization reaction of water $(\mathrm{OH^-}+\mathrm{H^+}\rightarrow\mathrm{H_2O})$ was found by various groups to proceed with an apparent large reaction distance of 6–8 Å as in Refs. 11, 33, and 107. Similar values of contact distance were found in studies of ground-state acid-base reactions[2,11,12] and in excited-state photoacid proton dissociation.[13,72–76,105]

Other possible reaction pathways for proton transfer, which may also take our observations into account, should also be considered. The proton may be transferred from the acid to the base concertedly through the solvent, or by moving sequentially in a von Grotthuss–type fashion (Fig. 16), through the hydrogen-bonding network connecting between the acid and base.[54] The first mechanism should be regarded as purely through solvent, without an additional inner step. The second mechanism contains at least one additional inner proton transfer stage, even though in this reaction scenario the acid and base, although connected by hydrogen bonds, are not in direct contact to each other, unlike we have outlined in Scheme 2.

The research of the various mechanisms by which the proton is transferred between proton acids and proton bases in aqueous solutions has been receiving important support from recent theoretical investigations. Ando and Hynes[108] studied the HF dissociation-recombination reaction and concluded in favor of a three-stage proton-transfer reaction. They have found the concerted reaction mechanism upon diffusional encounter to be energetically unfavorable compared to a stepwise proton-transfer reaction. A similar conclusion was drawn by the same authors in the study of HCl and HBr proton dissociation reaction.[41,109,110] Geissler *et al.*[35] showed that proton transfer along preexisting hydrogen bonds in water may be as fast as 100 fs even for the very weak acid H_2O. In the present study we have demonstrated that time-resolved IR spectroscopy is an exquisite tool towards achieving the goal of elucidating experimentally this long-standing paradigm of solution chemistry.

ACKNOWLEDGMENTS

The authors acknowledge support by the Deutsche Forschungsgemeinschaft (Project No. DFG NI 492/2-2), the German-Israeli Foundation for Scientific Research and Development (Project No. GIF 722/01), and the LIMANS Clus-

ter of Large Scale Laser Facilities (Project No. MBI000228). E.P. acknowledges the support from James Franck German-Israel Binational Program in laser-matter interaction.

[1] R. M. Noyes, Prog. React. Kinet. **1**, 129 (1961).
[2] A. Weller, Prog. React. Kinet. **1**, 187 (1961).
[3] J. B. Birks, *Photophysics of Aromatic Molecules* (Wiley-Interscience, London, 1970).
[4] U. M. Gösele, Prog. React. Kinet. **13**, 63 (1984).
[5] S. A. Rice, *Diffusion-limited Reactions*, edited by C. H. Bamford, C. F. H. Tripper, and R. G. Compton, Comprehensive Chemical Kinetics Vol. 25 (Elsevier, Amsterdam, 1985).
[6] J. Keizer, Chem. Rev. (Washington, D.C.) **87**, 167 (1987).
[7] M. Sikorski, E. Kristowiak, and R. P. Steer, J. Photochem. Photobiol., A **117**, 1 (1998).
[8] T. Förster, Z. Electrochem. **54**, 531 (1950).
[9] A. Weller, Z. Electrochem. **58**, 849 (1954).
[10] A. Weller, Z. Phys. Chem. (Leipzig) **17**, 224 (1958).
[11] M. Eigen, W. Kruse, and L. De Maeyer, Prog. React. Kinet. **2**, 285 (1964).
[12] M. Eigen, Angew. Chem., Int. Ed. Engl. **3**, 1 (1964).
[13] J. F. Ireland and P. A. H. Wyatt, Adv. Phys. Org. Chem. **12**, 131 (1976).
[14] M. Kuznetov and J. Ustrup, *Electron Transfer in Chemistry and Biology* (Wiley-Interscience, Chichester, 1999).
[15] G. Angulo, G. Grampp, and S. Landgraf, J. Inf. Rec. Mater. **25**, 381 (2000).
[16] R. M. Fuoss and C. A. Kraus, J. Am. Chem. Soc. **55**, 1019 (1933).
[17] M. N. Berberan-Santos and J. M. G. Martino, J. Chem. Phys. **95**, 1817 (1991).
[18] J. M. G. Martino, J. P. Farina, M. N. Berberan-Santos, J. Duhamel, and M. A. Winnik, J. Chem. Phys. **96**, 8143 (1992).
[19] R. Holzwarth, Methods Enzymol. **246**, 334 (1995).
[20] D. N. Silverman, Biochim. Biophys. Acta **1458**, 88 (2000).
[21] T. L. Nemzek and W. R. Ware, J. Chem. Phys. **62**, 477 (1975).
[22] D. D. Eads, B. G. Dismer, and G. R. Fleming, J. Chem. Phys. **93**, 1136 (1990).
[23] C. F. Shannon and D. D. Eads, J. Chem. Phys. **103**, 5208 (1995).
[24] J. R. Lakowicz, in *Topics in Fluorescence Spectroscopy*, edited by J. R. Lakowicz (Plenum, New York, 1994), Vol. 4, Chap. 5, pp. 293–337.
[25] M. von Smoluchowski, Z. Phys. Chem., Stoechiom. Verwandtschaftsl. **92**, 129 (1917).
[26] P. Debye, Trans. Electrochem. Soc. **82**, 265 (1942).
[27] K. M. Hong and J. Noolandi, J. Phys. Chem. **68**, 5 (1991).
[28] F. C. Collins and G. E. Kimball, J. Colloid Sci. **4**, 425 (1949).
[29] A. Szabo, J. Phys. Chem. **93**, 6929 (1989).
[30] L. Song, R. C. Dorfman, S. F. Swallen, and M. D. Fayer, J. Phys. Chem. **95**, 3454 (1991).
[31] G. Wilemski and M. Fixman, J. Chem. Phys. **58**, 4009 (1973).
[32] T. Yabe, H. Chosrowjan, K. Yamada, Y. Hirata, and T. Okada, J. Photochem. Photobiol., A **109**, 15 (1997).
[33] R. P. Bell, *The Proton in Chemistry*, 2nd ed. (Chapman and Hall, London, 1973).
[34] D. Marx, M. E. Tuckerman, J. Hutter, and M. Parrinello, Nature (London) **397**, 601 (1999).
[35] P. L. Geissler, C. Dellago, D. Chandler, J. Hutter, and M. Parrinello, Science **291**, 2121 (2001).
[36] W. Kühlbrandt, Nature (London) **406**, 569 (2000), and references therein.
[37] J. L. Skinner and H. P. Trommsdorff, J. Chem. Phys. **89**, 897 (1988).
[38] J. Leggett, S. Chakravarty, A. T. Dorsey, M. P. A. Fischer, A. Garg, and W. Zwerger, Rev. Mod. Phys. **59**, 1 (1987).
[39] P. Hänggi, P. Talkner, and M. Borkovec, Rev. Mod. Phys. **62**, 251 (1990).
[40] A. Oppenländer, C. Rambaud, H. P. Trommsdorff, and J.-C. Vial, Phys. Rev. Lett. **63**, 1432 (1989).
[41] K. Ando and J. T. Hynes, Adv. Chem. Phys. **110**, 381 (1999).
[42] T. Elsaesser, in *Ultrafast Hydrogen Bonding and Proton Transfer Processes in the Condensed Phase*, edited by T. Elsaesser and H. J. Bakker (Kluwer, Dordrecht, 2002), pp. 119–153.
[43] N. F. Scherer, L. R. Khundkar, R. B. Bernstein, and A. H. Zewail, J. Chem. Phys. **87**, 1451 (1987).
[44] N. F. Scherer, C. Sipes, R. B. Bernstein, and A. H. Zewail, J. Chem. Phys. **92**, 5239 (1990).
[45] M. Gruebele, I. R. Sims, E. D. Potter, and A. H. Zewail, J. Chem. Phys. **95**, 7763 (1991).
[46] R. Sims, M. Gruebele, E. D. Potter, and A. H. Zewail, J. Chem. Phys. **97**, 4127 (1992).
[47] P. Y. Cheng, D. Zhong, and A. H. Zewail, J. Chem. Phys. **103**, 5153 (1995).
[48] P. Y. Cheng, D. Zhong, and A. H. Zewail, J. Chem. Phys. **105**, 6216 (1996).
[49] M. F. Hineman, G. A. Brucker, D. F. Kelley, and E. R. Bernstein, J. Chem. Phys. **97**, 3341 (1992).
[50] J. A. Syage, J. Phys. Chem. **99**, 5772 (1995).
[51] S. K. Kim, J. J. Breen, D. M. Willberg, L. W. Peng, A. Heikal, J. A. Syage, and A. H. Zewail, J. Phys. Chem. **99**, 7421 (1995).
[52] D. Lührs, R. Knochenmuss, and I. Fischer, Phys. Chem. Chem. Phys. **2**, 4335 (2000).
[53] R. Knochenmuss and I. Fischer, Int. J. Mass. Spectrom. **220**, 343 (2002).
[54] C. Tanner, C. Manca, and S. Leutwyler, Science **302**, 1736 (2003).
[55] A. Douhal, S. K. Kim, and A. H. Zewail, Nature (London) **378**, 260 (1995).
[56] D. E. Folmer, L. Poth, E. S. Wisniewski, and A. W. Castleman, Jr., Chem. Phys. Lett. **287**, 1 (1998).
[57] E. Lenderink, K. Duppen, F. P. X. Everdij, J. Mavri, R. Torre, and D. A. Wiersma, J. Phys. Chem. **100**, 7822 (1996).
[58] M. Chachisvilis, T. Fiebig, A. Douhal, and A. H. Zewail, J. Phys. Chem. A **102**, 669 (1998).
[59] T. Fiebig, M. Chachisvilis, M. Manger, A. H. Zewail, A. Douhal, I. Garcia-Ochoa, and A. de La Hoz Ayuso, J. Phys. Chem. A **103**, 7419 (1999).
[60] S. Takeuchi and T. Tahara, Chem. Phys. Lett. **347**, 108 (2001).
[61] S. Murata, M. Nishimura, S. Y. Matsuzaki, and M. Tachiya, Chem. Phys. Lett. **219**, 200 (1994).
[62] S. Murata, S. Y. Matsuzaki, and M. Tachiya, J. Phys. Chem. **99**, 5354 (1995).
[63] S. Murata and M. Tachiya, J. Phys. Chem. **100**, 4064 (1996).
[64] O. Nicolet and E. Vauthey, J. Phys. Chem. A **106**, 5553 (2002).
[65] S. R. Keiding, D. Madsen, J. Larsen, S. K. Jensen, and J. Thøgersen, Chem. Phys. Lett. **390**, 94 (2004).
[66] T. Kobayashi, Y. Tagaki, H. Kandori, K. Kemnitz, and K. Yoshihara, Chem. Phys. Lett. **180**, 416 (1994).
[67] I. G. Rubtsov, H. Shirota, and K. Yoshihara, J. Phys. Chem. A **103**, 1801 (1999).
[68] S. Engleitner, M. Seel, and W. Zinth, J. Phys. Chem. A **103**, 3013 (1999).
[69] Q.-H. Xu, G. D. Scholes, M. Yang, and G. R. Fleming, J. Phys. Chem. A **103**, 10348 (1999).
[70] E. W. Castner, Jr., D. Kennedy, and R. J. Cave, J. Phys. Chem. A **104**, 2869 (2000).
[71] A. Morandeira, A. Fürstenberg, J.-C. Gumy, and E. Vauthey, J. Phys. Chem. A **107**, 5375 (2003).
[72] E. Pines, B.-Z. Magnes, M. J. Lang, and G. R. Fleming, Chem. Phys. Lett. **281**, 413 (1997).
[73] L. T. Genosar, B. Cohen, and D. Huppert, J. Phys. Chem. A **104**, 6689 (2000).
[74] B. Cohen, D. Huppert, and N. Agmon, J. Am. Chem. Soc. **122**, 9838 (2000).
[75] B. Cohen, D. Huppert, and N. Agmon, J. Phys. Chem. A **105**, 7165 (2001).
[76] E. Pines and D. Pines, in *Ultrafast Hydrogen Bonding and Proton Transfer Processes in the Condensed Phase*, edited by T. Elsaesser and H. J. Bakker (Kluwer, Dordrecht, 2002), pp. 155–184.
[77] N. P. Ernsting, S. A. Kovalenko, T. Senyushkina, J. Saam, and V. Farztdinov, J. Phys. Chem. A **105**, 3443 (2001).
[78] T. Elsaesser and W. Kaiser, Annu. Rev. Phys. Chem. **42**, 83 (1991).
[79] J. C. Owrutsky, D. Raftery, and R. M. Hochstrasser, Annu. Rev. Phys. Chem. **45**, 519 (1994).
[80] S. A. Kovalenko, N. Eilers-Konig, T. A. Senyushkina, and N. P. Ernsting, J. Phys. Chem. A **105**, 4834 (2001).
[81] S. A. Kovalenko, R. Schanz, H. Hennig, and N. P. Ernsting, J. Chem. Phys. **115**, 3256 (2001).
[82] S. Hogiu, W. Werncke, M. Pfeiffer, J. Dreyer, and T. Elsaesser, J. Chem. Phys. **113**, 1587 (2000).
[83] V. Kozich, W. Werncke, J. Dreyer, K.-W. Brzezinka, M. Rini, A. Kummrow, and T. Elsaesser, J. Chem. Phys. **117**, 719 (2002).
[84] V. Kozich, W. Werncke, A. I. Vodchits, and J. Dreyer, J. Chem. Phys. **118**, 1808 (2003).
[85] E. T. J. Nibbering, K. Duppen, and D. A. Wiersma, Chem. Phys. **183**, 167 (1994).

[86] G. R. Fleming and M. Cho, Annu. Rev. Phys. Chem. **47**, 109 (1996).
[87] W. P. de Boeij, M. S. Pshenichnikov, and D. A. Wiersma, Annu. Rev. Phys. Chem. **49**, 99 (1998).
[88] M. Rini, B.-Z. Magnes, E. Pines, and E. T. J. Nibbering, Science **301**, 349 (2003).
[89] R. P. Bell, *The Tunnel Effect in Chemistry* (Chapman and Hall, London, 1980), pp. 176–177.
[90] R. A. Marcus, J. Phys. Chem. **72**, 4249 (1965).
[91] A. O. Cohen and R. A. Marcus, J. Phys. Chem. **72**, 891 (1965).
[92] M. Eigen, in *Quantum Statistical Mechanics in the Natural Sciences*, edited by S. L. Minz and S. M. Wiedermayer (Plenum, New York, 1974), pp. 37–61.
[93] D. Shoup and A. Szabo, Biophys. J. **40**, 33 (1982).
[94] R. M. Fuoss, J. Am. Chem. Soc. **80**, 5059 (1958).
[95] D. Pines and E. Pines, J. Chem. Phys. **115**, 951 (2001).
[96] S. Y. Goldberg, E. Pines, and D. Huppert, Chem. Phys. Lett. **192**, 77 (1992).
[97] E. Pines and G. R. Fleming, Chem. Phys. **183**, 393 (1994).
[98] G. R. Fleming, *Chemical Applications of Ultrafast Spectroscopy* (Oxford University Press, Oxford, 1986).
[99] A. J. Cross, D. H. Waldeck, and G. R. Fleming, J. Chem. Phys. **78**, 6455 (1983).
[100] R. A. Kaindl, M. Wurm, K. Reimann, P. Hamm, A. M. Weiner, and M. Woerner, J. Opt. Soc. Am. B **17**, 2086 (2000).
[101] E. Pines, D. Pines, T. Barak, B.-Z. Magnes, L. M. Tolbert, and J. E. Haubrich, Ber. Bunsenges. Phys. Chem. **102**, 515 (1998).
[102] A. J. A. Aquino, D. Tunega, G. Haberhauer, and M. H. Gerzabek, J. Phys. Chem. A **106**, 1862 (2002).
[103] S. P. Porras, R. Kuldvee, S. Palonen, and M.-L. Riekkola, J. Chromatogr. A **990**, 35 (2003).
[104] R. Kuldvee, M. Vaher, M. Koel, and M. Kaljurand, Electrophoresis **24**, 1627 (2003).
[105] E. Pines, D. Huppert, and N. Agmon, J. Chem. Phys. **88**, 5620 (1988).
[106] G. Zundel, Adv. Chem. Phys. **111**, 1 (2000).
[107] W. C. Natzle and C. B. Moore, J. Phys. Chem. **89**, 2605 (1985).
[108] K. Ando and J. T. Hynes, J. Phys. Chem. A **103**, 10398 (1999).
[109] K. Ando and J. T. Hynes, J. Phys. Chem. B **101**, 10464 (1997).
[110] A. Al-Halabi, R. Bianco, and J. T. Hynes, J. Phys. Chem. A **106**, 7639 (2002).